Microbial Cell Factories

RESEARCH Open Access

Functional connexion of bacterioferritin in antibiotic production and morphological differentiation in *Streptomyces coelicolor*

Javier García-Martín[1], Laura García-Abad[1], Ramón I. Santamaría[1*] and Margarita Díaz[1*]

Abstract

Background Several two-component systems of *Streptomyces coelicolor*, a model organism used for studying antibiotic production in *Streptomyces*, affect the expression of the *bfr* (*SCO2113*) gene that encodes a bacterioferritin, a protein involved in iron storage. In this work, we have studied the effect of the deletion mutant Δ*bfr* in *S. coelicolor*.

Results The Δ*bfr* mutant exhibits a delay in morphological differentiation and produces a lesser amount of the two pigmented antibiotics (actinorhodin and undecylprodigiosin) compared to the wild type on complex media. The effect of iron in minimal medium was tested in the wild type and Δ*bfr* mutant. Consequently, we also observed different levels of production of the two pigmented antibiotics between the two strains, depending on the iron concentration and the medium (solid or liquid) used. Contrary to expectations, no differences in intracellular iron concentration were detected between the wild type and Δ*bfr* mutant. However, a higher level of reactive oxygen species in the Δ*bfr* mutant and a higher tolerance to oxidative stress were observed. Proteomic analysis showed no variation in iron response proteins, but there was a lower abundance of proteins related to actinorhodin and ribosomal proteins, as well as others related to secondary metabolite production and differentiation. Additionally, a higher abundance of proteins related to various types of stress, such as respiration and hypoxia among others, was also revealed. Data are available via ProteomeXchange with identifier PXD050869.

Conclusion This bacterioferritin in *S. coelicolor* (Bfr) is a new element in the complex regulation of secondary metabolism in *S. coelicolor* and, additionally, iron acts as a signal to modulate the biosynthesis of active molecules. Our model proposes an interaction between Bfr and iron-containing regulatory proteins. Thus, identifying these interactions would provide new information for improving antibiotic production in *Streptomyces*.

Keywords *Streptomyces*, Two-component systems, Antibiotic production, Bacterioferritin, Iron

*Correspondence:
Ramón I. Santamaría
santa@usal.es
Margarita Díaz
mardi@usal.es
[1]Departamento de Microbiología y Genética, Instituto de Biología Funcional y Genómica (IBFG), Consejo Superior de Investigaciones Científicas (CSIC), Universidad de Salamanca (USAL), C/ Zacarías González, nº 2, Salamanca 37007, Spain

Background

Streptomyces are Gram-positive filamentous bacteria that thrives in various environments, such as soil, where they are highly abundant. These bacteria belong to the phylum *Actinomycetota* (previously known as *Actinobacteria*) [1] and have a complex life cycle: a vegetative branched mycelium emerges from a spore, and, under adverse conditions, differentiates into a spore-producing aerial mycelium [2]. They possess a remarkable ability to synthesise industrial compounds, such as extracellular enzymes, and natural products such as antibiotics (*Streptomyces* produces approximately 80% of the antibiotics used) [3]. Furthermore, the production of these active molecules is controlled by intricate regulatory networks that link their development, environmental signals, and metabolism [4].

Trace metals act as signals that influence the development of microorganisms, with iron being an essential component in bacteria [5]. The relationship between iron homeostasis, antibiotic production, and morphological differentiation has been previously reported for the genus *Streptomyces* [5, 6]. It is known that iron deprivation triggers actinorhodin (ACT) production in *S. coelicolor* [7] and a null mutant of the siderophore receptor *desE* in this species exhibits altered morphological differentiation and ACT production [8]. The impact of iron on antibiotic production has also been described for other *Streptomyces* species, such as *S. hygroscopicus*, where niphimycin production is enhanced by high iron concentrations [9]. However, low iron concentrations drive exploratory growth, a new mode of *Streptomyces* development [10], and co-cultures of *Myxococcus* with other *Streptomyces* species increase their secondary metabolite expression due to iron scarcity [7]. Thus, several metabolites and processes are dependent on iron [11].

Additionally, several elements are responsible for iron homeostasis with functions related to uptake, storage, and detoxification, among others. As iron levels are usually low in the ecological niches of many bacteria, adaptive responses have been developed for the uptake of this essential resource [12–14]. For example, three different trishydroxamate siderophores (coelichelin, desferrioxamine E, and desferrioxamine B) share the role of acquiring ferric iron during the vegetative growth of *S. coelicolor* and *S. ambofaciens*. In *S. coelicolor*, desferrioxamines, and coelichelin biosynthesis, reception, and assimilation are carried out by the *desEFABCD* and *cchABCDEFEHIJ* clusters, respectively. Another siderophore importer is codified by *cdtABC* [8, 15]. Once ferric iron is inside the cell, owing to the work of chelators, it is reduced to ferrous iron to diminish its affinity for the siderophore and is released for its use in cellular metabolism [12].

Alternatively, ferrous iron is potentially toxic due to the Fenton reaction of ferrous ions with H_2O_2 which produces hydroxyl radicals. Therefore, cells store iron mainly in ferritins and bacterioferritins (Bfr) to avoid toxicity. Iron storage proteins take up iron in the soluble ferrous form, which is deposited in their central cavity in the oxidised ferric form. This reservoir can be used when external iron supplies are restricted [12, 16]. Therefore, iron sequestration is one of the main protection systems to counteract the effect of the iron-based Fenton reaction [17, 18].

In *S. coelicolor*, the bacterioferritin Bfr and three Dps proteins (*D*NA-binding *p*rotein from *s*tarved cells) have a putative function related to iron storage. The main role assigned to bacterioferritins is to store excess iron in conditions of metal abundance, and to release this iron in response to iron starvation [16, 17]. However, the specific physiological role of the *S. coelicolor* bacterioferritin remains to be elucidated. To date, it is known that the *S. coelicolor bfr* gene (*SCO2113*) is induced under osmotic stress by SigB (SCO0600) [19] and that the protein Bfr has been detected in extracellular vesicles of *S. coelicolor* together with other stress-related proteins [20]. Moreover, the three Dps proteins of *S. coelicolor* (DpsA, DpsB, and DpsC) play a role in nucleoid condensation in spore formation. However, they are not induced under oxidative stress conditions [21] as described for Dps in other bacteria [22]. DpsA and DpsC can oxidise ferrous iron and store it as ferric iron inside their cavities [23]. Also, HbpS, the accessory and sensory component of the two-component system SenS/R, provides an additional defence mechanism in the presence of iron [18, 24].

All bacterioferritins are heme-containing 24-mer proteins with a spherical structure of about 500 kDa. Typically, there are 12 hemes groups per 24-mer located at each of the 12 two-fold interfaces between units, which can bind 2000–3000 iron atoms per 24-mer [17, 25]. The crystal structure of several Bfr isolated from different microorganisms has been resolved [26, 27] including the Bfr from *S. coelicolor* (PDB ID:5XX9). By employing cryo-electron microscopy and crystallisation, Jobinchen et al. reported the iron mineralization inside *S. coelicolor* Bfr and proposed the importance of specific residues and heme groups in the internalisation and efflux of iron ions [28].

Overall, iron homeostasis must be strictly regulated to co-ordinate the availability of iron in each stage of cell development. In *S. coelicolor*, this regulation is mediated by two DtxR proteins, DmdR1 and Dmdr2, and the antiparallel gene *adm*. It has been proposed that the protein Adm may act as a repressor of antibiotic biosynthesis and is under the control of RpoZ, a sigma factor that connects development and secondary metabolism [29]. IdeR is the homologue of DmdR1 and DmdR2 in *S. avermitilis* and has pleiotropic regulatory functions that allow *S.*

avermitilis to adapt its growth in a complex environment in response to iron levels [30].

In previous work, we explored the regulatory network that triggers antibiotic production in *S. coelicolor* and the two-component systems (TCSs) responsible for signal transduction that act as global regulators of this production [31, 32]. Specifically, for *bfr*, we know that this gene is a direct target of AbrC3, a positive antibiotic response regulator characterized by our group [33]. Moreover, the expression of *bfr* is altered in null mutants of other studied TCSs, such as the orphan regulator Aor1 and the TCS AbrB1/B2 [34, 35].

In this work, a phenotypic study of a *bfr* deletion mutant in *S. coelicolor* is described, demonstrating the importance of the Bfr protein in antibiotic and morphological differentiation across different culture media. We also report a proteomic comparative study between this mutant and the wild-type strain, revealing significant proteomic changes observed in the *bfr* mutant and highlighting the role of Bfr under oxidative stress conditions. Moreover, we analysed the relationship between iron homeostasis and development in both the wild type and *bfr* mutant. Our results indicate that Bfr, and by extension iron homeostasis, is crucial for activating the regulatory network responsible for antibiotic production and morphological differentiation.

Methods

Strains, media, and growth conditions

Escherichia coli DH5α and ET12567 (a dam$^-$ strain) were utilised to obtain DNA for transforming *S. coelicolor*. *E. coli* ET12567 (pUZ8002) [36] was used to transfer a pCRISPR plasmid derivative to *S. coelicolor* M145. For the antibacterial activity assay, *E. coli* DH5α, *Staphylococcus epidermidis* ATCC 14,990, and *Micrococcus luteus* CECT 245 were employed and grown on LB [37], BHI (Condalab, REF 1400), and YEPD [38], respectively. *Bacillus subtilis* (CECT 4522) was grown as an overlay on NA from Scharlau (Scharlab, S. L., REF 02-140) for the CDA bioassay [34].

For the phenotypic assays, *S. coelicolor* M145 (prototroph; SCP1$^-$, SCP2$^-$) and its Δ*bfr* mutant strain were grown on modified NMMP [39], containing 4.5 mM NaH_2PO_4/K_2HPO_4 buffer pH 6.8 and three different iron concentrations (10 nM, 4 µM, and 2 mM), and the complex solid media YEPD, LB, R2YE, and MSA. R2YE was also used for transformation purposes, MSA for sporulation [40], and YEPD or LB for colony forming unit (CFU) quantification. NA was used for the CDA and coelymicin production assays. LB medium and NMMP, containing the three iron concentrations tested, were used for antibiotic quantification and for measuring iron and reactive oxygen species (ROS) levels. Proteomic experiments were performed on LB. TSB medium (Condalab, REF 1224) was used for pCRISPR-derived plasmid loss and DNA extraction.

Iron was added to sterilised NMMP medium using a freshly prepared and filtered 100 mM $FeSO_4$ stock in 10 mM HCl to prevent oxidation [41]. When necessary, the media were supplemented with antibiotics: *E. coli* media - ampicillin (100 µg mL^{-1}), apramycin (50 µg mL^{-1}), kanamycin (50 µg mL^{-1}), chloramphenicol (25 µg mL^{-1}), or nalidixic acid (25 µg mL^{-1}) and *S. coelicolor* media - neomycin (20 µg mL^{-1}) or apramycin (15 µg mL^{-1}).

DNA manipulation and plasmid construction

Plasmid isolation, restriction enzyme digestion, ligation, and transformation of *E. coli* and *S. coelicolor* were conducted using the methods by Green et al. [42], and Kieser et al. [40], respectively. The plasmids used are listed in Additional File S1.

The *bfr* gene, along with its promoter, was amplified by PCR using oligonucleotides LGA001/LGA002 and genomic DNA from *S. coelicolor* M145 as the template. The 770-bp fragment was cloned into pKC796 [43] at a BamHI site yielding the integrative plasmid pKC796-Bfr. The same DNA amplicon (*bfr* and its promoter) was cloned into the multicopy plasmid pN702GEM3 [44], resulting in the pN-Bfr overexpression plasmid. Genomic DNA from *S. coelicolor* was extracted after grown in TSB cultures [45].

Mutant construction

To delete the *bfr* gene using the CRISPR/Cas9 system, a single guide RNA (sgRNA) comprising 20 *bfr* specific nucleotides, GCAGGACACGGATCGTCATA, was designed using the web resource CRISPy [46, 47]. Using the pCRISPR-Cas9 [48] as the DNA template and primers SAM-051 and MTS-014 (Additional File S2), the whole sgRNA was amplified by PCR. This fragment was cut with NcoI and SnaBI enzymes and inserted into pCRISPR-Cas9, digested with the same enzymes, to generate pCRISPR-Cas9-sgBfr. Additionally, 1 kb to the left and 1 kb to the right of *bfr* gene were amplified using genomic *S. coelicolor* M145 DNA and cloned into the plasmid containing sgRNA to be used as a template for repairing Cas9 cuts through homologous recombination. The 1-kb fragment upstream of the *bfr* gene (left, primers SAM-046/SAM-047) (Additional File S2), and 1 kb downstream (right, primers SAM-048/SAM-049) (Additional File S2) were amplified. These DNA fragments were used as the template in an overlapping PCR using SAM-046/SAM-049 primers. The resulting DNA fragment was digested with NheI, which produces sticky ends when cut with XbaI, and introduced into the XbaI site of the pCRISPR-Cas9-sgBfr to generate the final pCRISPR-Cas9-Bfr plasmid. All plasmids were sequenced and verified.

The three plasmids, the empty one (pCRISPR-Cas9), the one harbouring only the sgRNA (pCRISPR-Cas9-sgBfr), and the final plasmid with the guide and the template (pCRISPR-Cas9-Bfr) were introduced into *E.coli* ET12567 pUZ8002. Then, all three were transferred to *S. coelicolor* by interspecific conjugation [36] and apramycin-resistant colonies were selected. To induce the loss of the plasmids (which were thermosensitive), the colonies obtained were grown in liquid TSB under agitation (200 rpm) at 37 ºC for 2 days. Apramycin-sensitive colonies were again selected.

Genomic DNA was obtained from the *S. coelicolor* wild-type strain and putative M145 *Δbfr* mutant colonies and the correct deletion of *bfr* gene was verified by PCR using outer primers (OP: LGA-012/LGA-013) and inner primers (IP: LGA-010/LGA-011) (Additional File S3).

Growth and antibiotic production analysis

Phenotypic studies were conducted on plates containing various solid media, inoculated with 5×10^5 spores added in a 5 µL drop and incubated at 30 ºC for several days. The plates were monitored for changes in colour in the colonies formed and in the culture medium, as well as for morphology changes. Under standard conditions, RED antibiotic production can be detected after two days as red colonies, ACT production as a blue halo around the colonies, and aerial mycelium and spores appear white and grey, respectively. All assays were performed in triplicate.

Growth was assayed using liquid LB medium cultures (10 mL) inoculated with 4×10^6 spores mL^{-1} grown at 28 ºC under agitation (200 rpm). The growth rate was determined by measuring the dry weight of the cultures in triplicate.

ACT and RED antibiotic production were quantified from liquid cultures (10 mL of medium with 4×10^6 spores mL^{-1} incubated at 28 ºC) using the spectrophotometric method described in Yepes et al., 2011 [49]. All experiments were conducted in quadruplicate and measures were normalised by cellular dry weight.

CDA was detected as previously described [34]. Colonies of *S. coelicolor* M145 and *Δbfr* strains, originating from a 5-µL drop containing 5×10^5 spores, were grown on NA for 3 days at 30 ºC. A 5-mL overlay with *Bacillus subtilis* (0.2 mL, OD 0.25) in soft NA (0.5% agar) and 70 mM $Ca(NO_3)_2$ was added. The same overlay without $Ca(NO_3)_2$ was used as a negative control. The plates were incubated for an additional day at 30 ºC. The inhibition halo produced by adding Ca^{2+} was measured and compared between the two strains. This experiment was performed in triplicate.

Coelimycins were detected on solid NA supplemented with 300 mM of glutamic acid as previously described [50]. The pH was adjusted to 7.2 using NaOH. Colonies and patches of *S. coelicolor* M145 and *Δbfr* strains with 5×10^5 spores were cultivated on solid NA containing 300 mM Glu for 3 days at 30 ºC. Coelimycins were observed as a yellow halo around the colonies. This experiment was done in quadruplicate.

Iron quantification

S. coelicolor M145 and *Δbfr* strains were grown in liquid LB for 5 days or NMMP containing different iron concentrations (10 nM, 4 µM, and 2 mM) for 8 days. Samples of 300 µL of mycelium were collected, washed twice with 10.3% sucrose, and frozen at – 20 ºC. Labile and total cellular iron were quantified using a colorimetric assay with ferene-S (Sigma, REF 82940) and modified using previously described protocols [51, 52].

Labile iron

Cellular pellets were lysed using a fresh lysis buffer (25 mM Tris pH 8.0, 10.3% sucrose, 3 mg mL^{-1} lysozyme) and incubated for 2 h at 37 ºC. A total of 500 µL of freshly prepared labile iron detection reagent (5 mM ferene-S and 10 mM ascorbic acid in 2.5 M ammonium acetate buffer pH 4.5) were added. After incubation for 30 min at 25 ºC, the samples were centrifuged for 15 min at 1500 g and the absorbance of ferene-Fe^{2+} complexes was measured at 564 nm.

Total iron

Cellular pellets were mixed with 500 µL of freshly prepared digestion reagent (2,25% w/v $KMnO_4$, 5% v/v HCl) by vortexing and incubated for 4 h at 65 ºC [53]. After 30 min at room temperature, cooled samples were treated with 500 µL of freshly prepared total iron detection reagent (5 mM ferene-S and 1 M ascorbic acid in 2.5 M ammonium acetate buffer pH 4.5) and incubated for 30 min at 25 ºC. Then, they were centrifuged for 15 min at 1500 g and the absorbance of the supernatant was measured at 564 nm.

Calibration curves were made using freshly prepared $FeCl_3$ standards (0.5–50 nmol) for both protocols. Measurements were made in quadruplicate and normalised by cellular dry weight.

Antibiogram assay

Three microorganisms were tested: *E. coli* on LB, *S. epidermidis* on BHI, and *M. luteus* on YEPD. Square Petri dishes (12×12 cm) containing 70 mL of medium were prepared with an overlay of 10 mL of soft agar (0.5%) and each microorganism (0.4 mL, OD 0.2). Plugs of NMMP (10 nM, 4 µM, and 2 mM iron) containing colonies (5×10^5 spores) of *S. coelicolor* M145 and *Δbfr* were obtained using a cork borer (0.7 cm in diameter) and assayed on the plates containing the lawn of microorganisms tested. Plates were incubated for 4 h at 4 ºC for

antibiotics diffusion and then incubated for 2 days at 30 ºC. The resultant inhibition halos were measured. Bioassays were done in triplicate.

Quantitative proteomics

Samples of 10^6 spores of *S. coelicolor* M145 and *Δbfr* were grown over a cellophane disk (8 cm in diameter) deposited on the surface of solid LB medium for 3 and 4 days. Mycelium was collected using a sterilized spatula and washed twice with 10.3% sucrose. The entire process was performed with the samples on ice. The pellets were resuspended in 400 µL of protein extraction buffer (0.1 M Tris-HCl pH 7, 5 mM DTT, 6 M urea, 2 M thiourea, 1% CHAPS and protease inhibitor cocktail tablets *cOmplete* [Roche, REF 11 697 498 001] following manufacturer indications) and vortexed. The proteins were extracted by carrying out 4 cycles of sonication (10 min 30 s ON and 30 s OFF, high intensity) in a *Bioruptor® Standard* (Diagenode) sonication system at 4 ° C. Four biological replicates were extracted from each strain.

The quantity of proteins from the resultant extracts was observed on SDS-PAGE and measured using the Quick Start Bradford Dye Reagent (BIO-RAD, REF 5000205) assay. The Functional Proteomics facility at the Spanish National Centre for Biotechnology (CNB, CSIC, Madrid, Spain) [54] performed the quantitative proteomic experiment using peptide fractionation and TMT labelling. The mass spectrometry proteomics data have been deposited to the ProteomeXchange Consortium [55] via the PRIDE [56, 57] partner repository with the dataset identifier PXD050869 and https://doi.org/10.6019/PXD050869.

The proteins identified and quantified with an adjusted p-value < 0.05 were analysed using the StrepDB [58], STRING database [59, 60], and *Cytoscape* software v 3.10.1 [61]. Protein function was studied using databases such as Google Scholar [62], UniProt [63, 64], NCBI Conserved Domain Database [65, 66], Kyoto Encyclopedia of Genes and Genomes (KEGG) [67, 68], and Database for Annotation, Visualization and Integrated Discovery (DAVID) [69, 70].

Oxidative stress tolerance

Previous assays were adapted to test colony survival after oxidative stress treatment [71, 72]. Samples containing 10^6 spores of *S. coelicolor* M145 and *Δbfr* were resuspended in germination medium (1.11 g/L $CaCl_2$, 10 g/L casamino acid, 10 g/L yeast extract) [39] and heat shocked for 10 min at 50 ºC. The spores were then treated with four H_2O_2 concentrations (0, 4, 8, and 20 mM) for 30 min at 30 ºC, washed twice with 10.3% sucrose, resuspended in new germination medium, and incubated for 3 h at 30 ºC. The cells were diluted 1:1000 and plated on LB solid medium. After three days, colony forming units (CFU) were counted and the survival ratio was calculated as the ratio between the number of colonies originating from the treated cells and the control cells. This experiment was carried out in quadruplicate.

Reactive oxygen species measurement

Reactive oxygen species (ROS) were measured from 10 mL-liquid cultures, containing 5×10^5 spores mL^{-1} of both *S. coelicolor* M145 and *Δbfr* strains incubated at 28 ºC under agitation (200 rpm), and on 10 mL of LB and NMMP supplemented with 10 nM, 4 µM and 2 mM of iron. Afterwards, 2',7'-dichlorofluorescin diacetate (DCFH2-DA, Sigma, REF D6883) was added to each flask to a final concentration of 10 µM and the cultures were incubated in the dark for three hours. The rest of the process from this point was performed in the dark or minimum light conditions. The mycelium was washed twice with 10.3% sucrose, resuspended in 500 µL of 10.3% sucrose, and lysed using 1–1.15 mm glass beads *Glasperlen* (B. Braun Melsungen Apparatebau, REF 05861/711) in a *FastPrep™ FP120* cell disruption system (Savant BIO 101) (4 cycles of 15 s at high intensity). Then, 100 µL of each supernatant were dispensed into a 96-well F-bottom microplate and the fluorescence ($\lambda_{excitation}$ = 485 nm, $\lambda_{emission}$ = 530 nm) was measured in a *Varioskan® Flash* reader (Thermo Scientific). Four biological replicates were measured in triplicate. The fluorescence units were normalized by protein quantification by Bradford assay.

Iron chelators assay

LB medium supplemented with increasing concentrations (0, 50, 100, 200, and 300 µM) of 2,2'-bipyridyl (BIP) (Sigma, REF D216305) and bathophenanthrolinedisulfonic acid (BPS) (Sigma, REF 146617) was dispensed into Sterillin™ 25 well 100 mm plates (Bibby Sterilin Ltd, Stone, Staffs, UK). Colonies of *S. coelicolor* M145 and *Δbfr* containing 5×10^5 spores were cultivated at 30 ºC. A phenotypic analysis was carried out for 7 days and the colonies were cultivated in quadruplicated.

Statistical analysis

All statistical analyses were performed using the *GraphPad Prism* software v 8.0.1 (GraphPad Software, San Diego, CA, USA). Data are shown as mean ± SEM. The normality of data sets was checked using the Shapiro-Wilk test. Two-way ANOVA (for experiments with two factors such as iron concentration and strain) with Holm-Šídák test for multiple comparisons (following software recommendations), and t-tests (for experiments with only two sets of measurements) were performed. Statistical differences are represented using one ($p < 0.05$) or two ($p < 0.01$) asterisks.

The statistical analysis of the quantitative proteomic data was performed by the Functional Proteomics facility

at the Spanish National Centre for Biotechnology using Proteome Discoverer software v2.5.

Results

Bfr plays a key role in antibiotic production and differentiation in *S. coelicolor* M145

The *bfr* gene (*SCO2113*) encoding a bacterioferritin (Bfr) was deleted from *S. coelicolor* M145 using CRISPR-Cas9 technology [48] and the plasmid pCRISPR-Cas9-Bfr. The correct deletion of the *bfr* gene was verified (see *Methods*) (Additional File S3).

The phenotypes of the mutant *Δbfr* were compared with those of the wild-type (M145) strain on various rich solid media: MSA, LB, R2YE, and YEPD (Fig. 1). No clear phenotypic differences were observed on MSA for either strain. In contrast, the *Δbfr* mutant exhibited a strong phenotype on the other three complex media: LB, R2YE, and YEPD. On these media, the following changes were observed: ACT production was almost completely inhibited, RED production was delayed, and cellular differentiation did not result in the formation of aerial mycelium in the mutant strain (Fig. 1A). Furthermore, all these *Δbfr* strain phenotypes were complemented by the integrative plasmid pKC796-Bfr on LB and R2YE (Fig. 1B). Therefore, the absence of bacterioferritin was detrimental to antibiotic production and differentiation on these complex media.

Since LB medium presented the clearest and most reproducible phenotypes for the strains, it was also used for liquid growth assays and antibiotic quantification. For *Δbfr*, RED (Fig. 2A), and ACT (Fig. 2B) production was severely diminished when grown in LB liquid medium and the differences detected between the wild-type and mutant strains were significant. Strikingly, the decreased antibiotic production observed for the strain lacking Bfr was accompanied by a significantly increased growth rate compared to the wild type (Fig. 2C). In fact, the spores of strain *Δbfr* incubated at 28 °C germinated at 8 h, while in the wild type, the germination tube was not clearly visible until 10 h. In addition, mycelia did not present any phenotypic alterations further along the growth curve (Fig. 2D).

Overexpression of the *bfr* gene does not affect *S. coelicolor* M145 development

Since the deletion of *bfr* resulted in reduced antibiotic production compared to the wild type, the effect of overexpressing the *bfr* gene was also studied. The *bfr* overexpression plasmid, pN-Bfr, and the empty vector, pN702GEM3, were transformed in *S. coelicolor* M145. All transformants obtained for both strains were grown

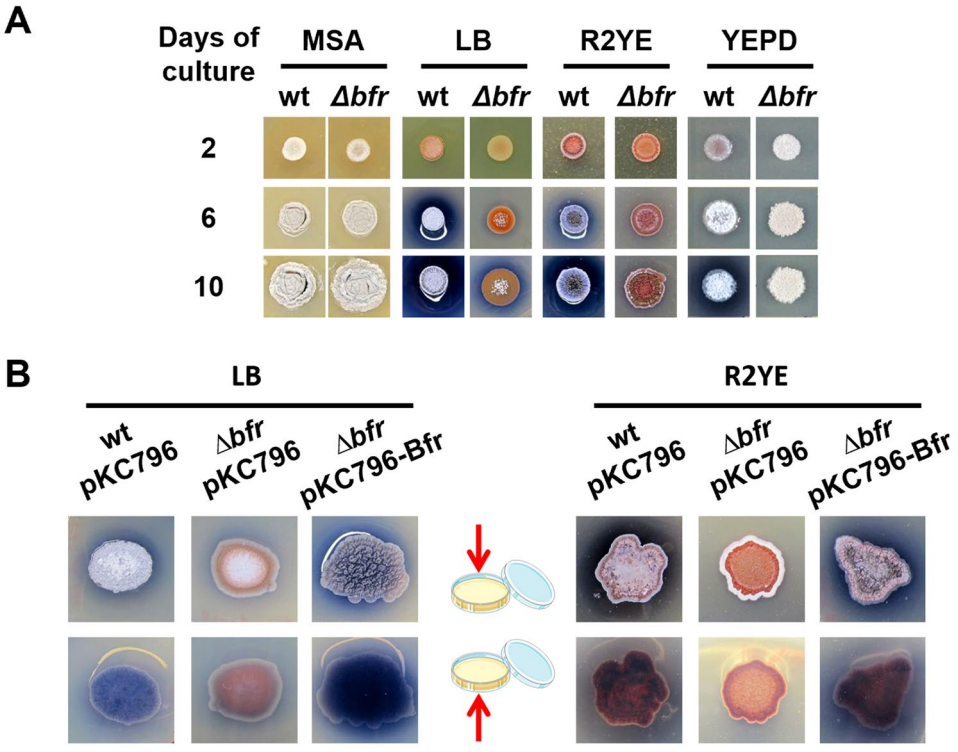

Fig. 1 Δ bfr phenotype and complementation. (**A**) Comparison of antibiotic production and differentiation of *S. coelicolor* M145 wild-type strain with its *Δbfr* mutant growing for 2, 6, and 10 days on several media (MSA, LB, R2YE, and YEPD). (**B**) Complementation of *S. coelicolor Δbfr* mutant with the integrative plasmid pKC796-Bfr after 6 days on LB (left) and R2YE (right) media. The wild type (wt) and *Δbfr* carrying the empty plasmid pKC796 were used as controls

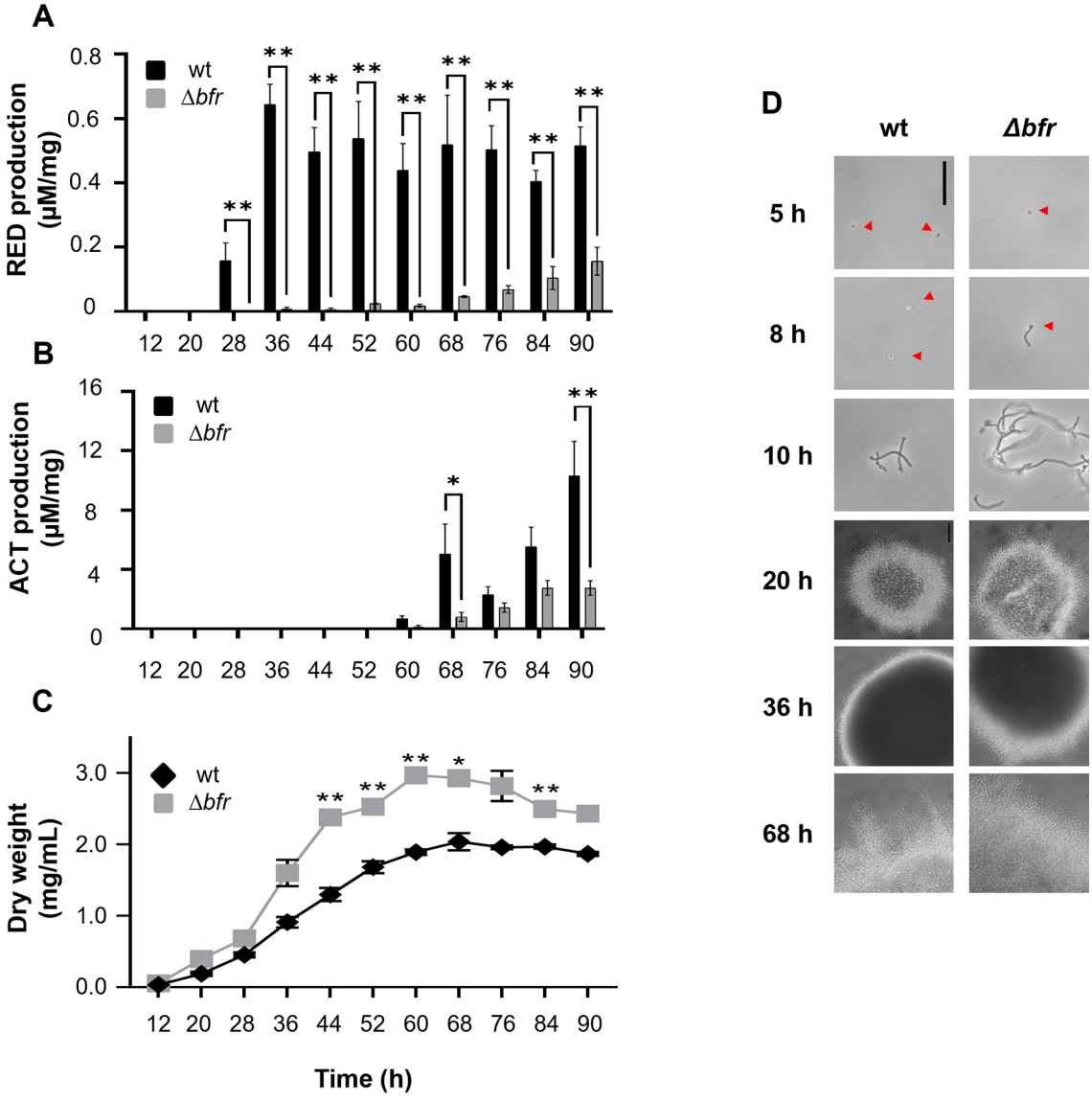

Fig. 2 Δ bfr antibiotic production and growth rate in liquid medium. *S. coelicolor* M145 wild type (wt) is represented in black and the *Δbfr* mutant in grey. Error bars show the standard error of the mean of the experiments carried out in quadruplicate. Asterisks show statistical differences between the two strains at each time point: *: $p < 0.05$; **: $p < 0.01$ (two-way ANOVA). (**A**) RED production in μM/mg at several time points in the growth curves in LB. (**B**) ACT production in μM/mg at several time points in the growth curves in LB. (**C**) Growth curves of *S. coelicolor* M145 and *Δbfr* mutant in LB. (**D**) Germination of spores (red triangles) and mycelia of *Δbfr* and wt at different culture times under an optical microscope. Bar: 300 μm

on LB, R2YE, and YEPD media supplemented with neomycin.

The overexpression of *bfr* on solid media did not significantly affect the final development of *S. coelicolor* (7 and 10 days) on any of the media assayed, although a slight delay in aerial mycelium formation was observed at 3 days (Additional File S4A). Additionally, less ACT was produced on YEPD at 10 days (Additional File S4 A). Liquid cultures in LB with neomycin were used to quantify ACT and RED production. Spores from *S. coelicolor* M145 harbouring pN702GEM3 and pN-Bfr plasmids were obtained and used as the inoculum. No statistical differences between the two strains were detected, except that the control strain with the empty plasmid (pN702GEM3) produced more RED than the strain overexpressing *bfr* (pN-Bfr) at day 3 (Additional File S4B).

Does iron concentration affect antibiotic production and differentiation in *S. coelicolor* M145 and its mutant strain Δbfr?

Bfr proteins, including Bfr from *S. coelicolor*, are implicated in Fe metabolism [17, 28]. Thus, we set out to test whether different iron concentrations could influence antibiotic production and/or differentiation, and if any

arising effect would occur differentially between the two strains, i.e., wild type and the mutant. For this purpose, minimal NMMP liquid and solid media with a standard concentration of Fe (4 µM), a low concentration (10 nM), and a high concentration (2 mM), were used for this experiment.

In liquid NMMP medium (Additional File S5), RED and ACT production was quantified every 2 days for 8 days. The results from these liquid cultures are shown in Fig. 3A and Additional File S6. In NMMP with 10 nM iron, RED production was higher in M145, with no statistically significant differences found (Fig. 3A left). Additionally, there was hardly any ACT produced in *Δbfr* but

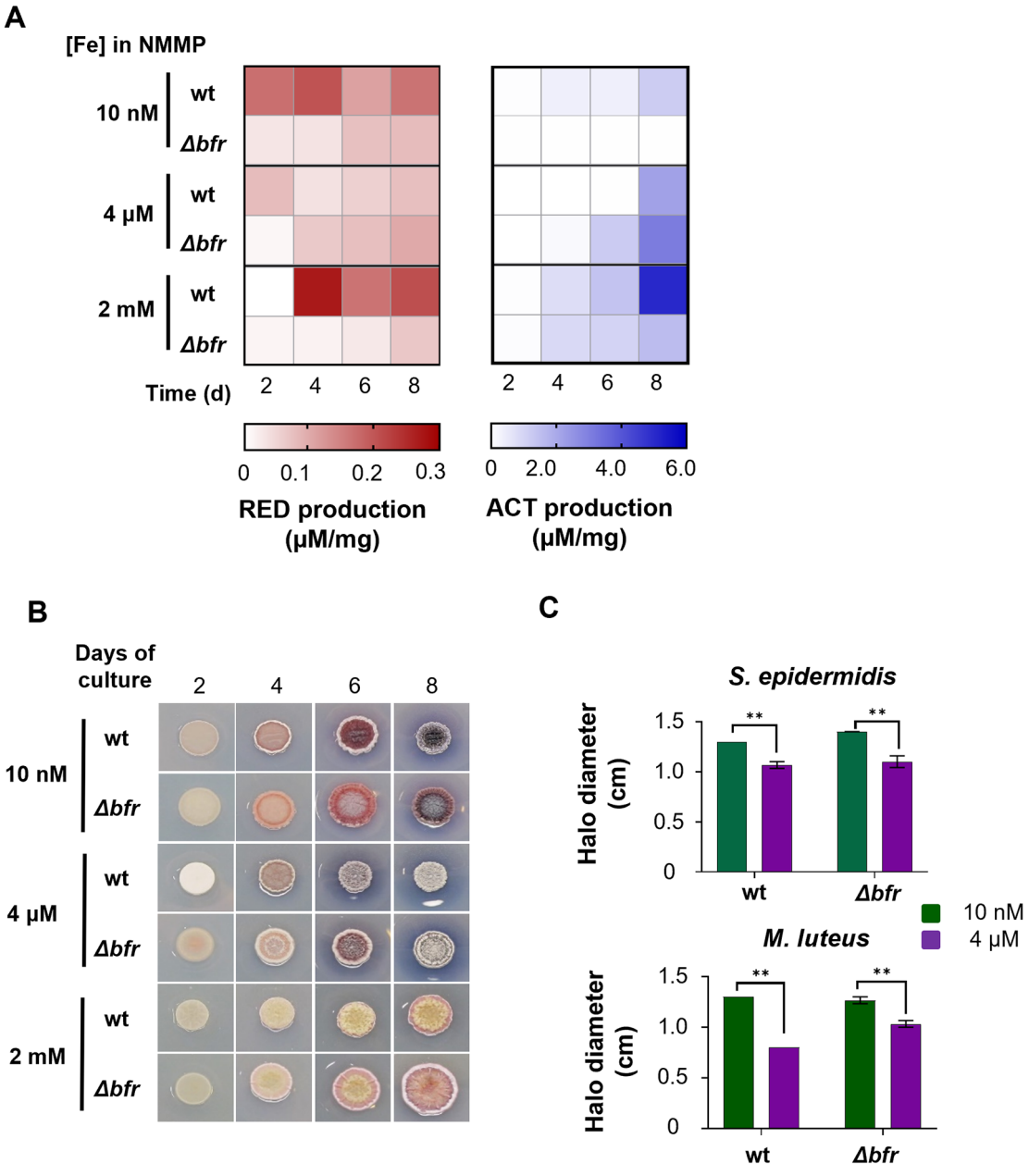

Fig. 3 Effect of iron concentration in NMMP medium cultures of *S. coelicolor* M145 and Δ *bfr.* (**A**) RED and ACT quantification of liquid cultures in NMMP with an iron concentration of 10 nM, 4 µM, and 2 mM in µM/mg of *S. coelicolor* M145 (wt) and Δ*bfr*. (**B**) The phenotype of colonies (5×10^5 spores) of *S. coelicolor* M145 (wt) and Δ*bfr* on solid NMMP with 10 nM, 4 µM and 2 mM of iron. (**C**) Measurement of halo diameters of the antibiogram against *S. epidermidis* and *M. luteus* using plugs of *S. coelicolor* M145 (wt) and Δ*bfr* (colonies of 5×10^5 spores) grown on NMMP with 10 nM and 4 µM of iron. Error bars show the standard error of the mean of the experiments carried out in triplicate. Asterisks show statistical differences between the two strains at each time point: *: $p < 0.05$; **: $p < 0.01$ (two-way ANOVA)

a low amount in M145 (about 1.2 μM mg^{-1}) (Fig. 3A right). In NMMP with 4 μM iron, RED production was similar in both strains (Fig. 3A left). However, in the mutant, ACT was produced earlier, at day 6, as compared to the wild type, and was even greater at day 8 (Fig. 3A right). Lastly, in NMMP with 2 mM iron, RED production in *Δbfr* was approximately half than in M145 (which produces 0.27 μM mg^{-1} at day 4 and 0.21 μM mg^{-1} at day 8). ACT production in the mutant remained constant starting from day 4 (1.58 μM mg^{-1} at day 8); however, M145 presented the highest ACT (5.04 μM mg^{-1} at day 8) production in this iron concentration. As shown in Additional File S6, all differences in the quantifications of antibiotic production were statistically significant according to the ANOVA analysis.

On solid media, antibiotic production and differentiation of the colonies were observed for 8 days (Fig. 3B). On NMMP with 10 nM iron, both strains produced almost no white aerial mycelium but could produce RED and ACT. On NMMP with 4 μM iron, there were no clear differences between strains, but *Δbfr* produced more ACT at day 8 (seen as a bigger blue halo), similar to its increased production detected in liquid medium (in this case at day 6). Finally, on NMMP with 2 mM iron, neither M145 nor *Δbfr* produced aerial mycelia and ACT production (blue halo) was not observed. Nonetheless, M145 produced yellow vegetative mycelia, whereas those of *Δbfr* remained red.

These results show that iron affects secondary metabolism and development in *S. coelicolor* M145 and *Δbfr*, and, under the tested conditions, this effect is different in solid and liquid media. Although it has been described that low iron concentrations enhance ACT production [7], under our experimental conditions, micromolar iron concentrations accelerated ACT production in *Δbfr*, while millimolar concentrations of iron, which enhance antibiotic production in M145 in liquid medium, blocked antibiotic production and differentiation in both strains grown on solid medium.

In addition, the antibiotic activity against three microorganisms (*S. epidermidis*, *M. luteus*, and *E. coli*) of the wild type and the *Δbfr* mutant strain grown on solid NMMP medium, with 10 nM, 4 μM and 2 mM of iron, was also tested using an antibiogram assay (Fig. 3C and Additional File S7). No antibiotic activity against *E. coli* was detected in any of the conditions tested. The activity against the two Gram-positive bacteria was stronger in cells grown on NMMP with 10 nM iron for the two strains. Moreover, *Δbfr* grown on NMMP with 4 μM iron had stronger antibiotic activity against *M. luteus* than the wild type. Neither M145 nor *Δbfr* showed antibiotic activity when they were grown on NMMP with 2 mM iron. This experiment showed that iron restriction enhanced the antibiotic activity of *S. coelicolor* and that this effect was independent of the presence of the *bfr* gene.

Differences between M145 and Δbfr strains are not due to changes in intracellular iron concentrations

The phenotypic differences observed in antibiotic production and morphogenesis between the wild type and *Δbfr* strain (as mentioned above) could be attributed to changes in the pool of labile iron (iron not incorporated into macromolecules) and/or in total iron concentration (all the iron inside the cell, free or associated with macromolecules) due to the absence of the Bfr storage protein. Therefore, both labile and total intracellular iron concentrations were measured in liquid cultures of both strains grown in 10 nM, 4 μM and 2 mM NMMP media.

Intracellular iron concentrations from cultures of both strains in NMMP with 10 nM iron were too low to obtain any reliable measurements. There were no statistically significant differences between the strains in the other two media (4 μM and 2 mM). The *Δbfr* mutant had a higher labile iron content on days 4 and 6 in NMMP with 4 μM iron, and the total iron levels were similar to labile iron in this medium (values about 0.1–0.35 nmol mg^{-1}) (Fig. 4A). However, iron levels were much higher in NMMP with 2 mM iron and total iron concentration was about twice as high as the labile iron concentration (Fig. 4B).

This experiment was also conducted in LB medium (which contains about 17 μM iron [73]), where the *Δbfr* phenotypes were more notable. As growth in rich media is faster for both strains, we measured the iron concentrations on days 2, 3, 4, and 5. The labile and total iron levels (about 0.25–0.5 nmol mg^{-1}) were comparable to those obtained in NMMP with 4 μM iron and there were no statistically significant differences in iron levels between the two strains in LB (Fig. 4C).

In conclusion, despite the iron storage capacity of Bfr, the lack of this protein, in *S. coelicolor*, does not alter the levels of total or labile intracellular iron.

Different iron chelators alter development in *S. coelicolor* M145 and Δbfr

Lee et al. reported a similar effect on ACT activation by reducing the concentration of iron in the culture medium and by using BIP as an iron chelator [74]. We aimed to investigate whether iron chelators could affect *S. coelicolor* M145 and *Δbfr* when grown on LB, the complex medium used for antibiotic quantification. Two iron chelators were employed: BIP, which is permeable and sequesters both extracellular and intracellular iron, and BPS, which cannot enter the cell and only sequesters extracellular iron [75].

The results obtained for BIP are shown in Fig. 5A. In the wild type M145, ACT production decreased as the

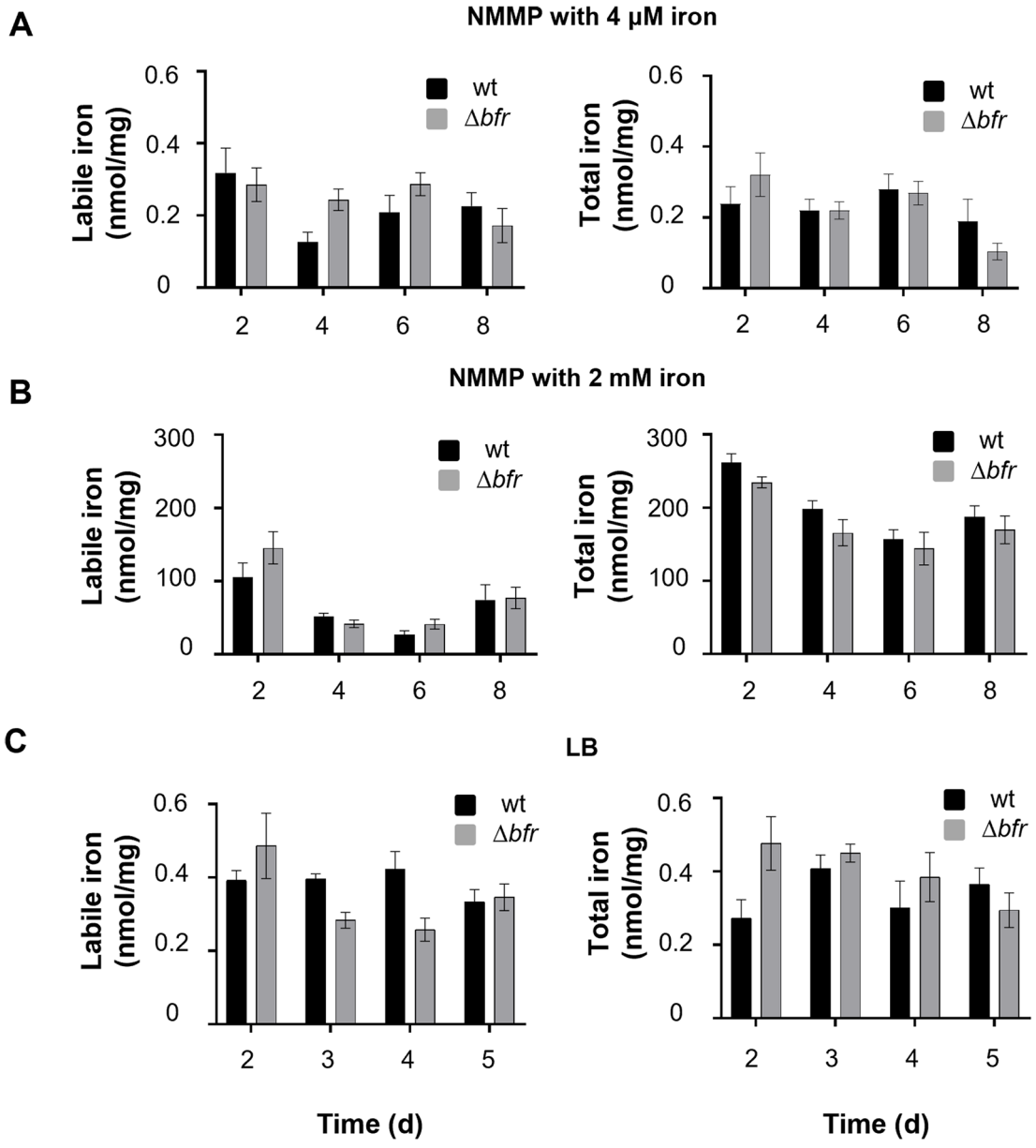

Fig. 4 Iron levels in liquid cultures of *S. coelicolor* M145 and Δ *bfr*. Labile (left) and total (right) iron quantification in NMMP with 4 µM iron (**A**), NMMP with 2 mM iron (**B**), and LB (**C**) in nmol/mg. Error bars show the standard error of the mean of the experiments carried out in quadruplicate. Two-way ANOVA was performed for statistical analysis

BIP concentration in the medium increased. Differentiation was slightly delayed with 100 µM BIP, and aerial mycelia formation was blocked with 200 µM. Differentiation and antibiotic production were abolished with 300 µM BIP. In the *Δbfr* mutant, some aerial mycelia were induced with the BIP treatment (higher concentration equates to less aerial mycelium formation). Normal red colouration was delayed with 200 µM BIP and, at the highest concentration tested (300 µM), the mutant phenotype was similar to that of the wild type, with no differentiation or antibiotic production.

As shown in Fig. 5B, BPS had a stronger negative effect on differentiation for M145 at 3 and 4 days. BPS delayed aerial mycelium formation, and ACT production was slightly lower with 100 µM BPS, although this could be a consequence of the delay in differentiation. The two highest concentrations (200 and 300 µM) blocked white aerial hyphae formation, and M145 produced a vegetative mycelium with a dark border, with ACT production and a darker colour in 200 µM BPS. For the *Δbfr* mutant, some aerial mycelium and ACT production were observed at days 6 and 7 with 50 µM BPS, but for the rest

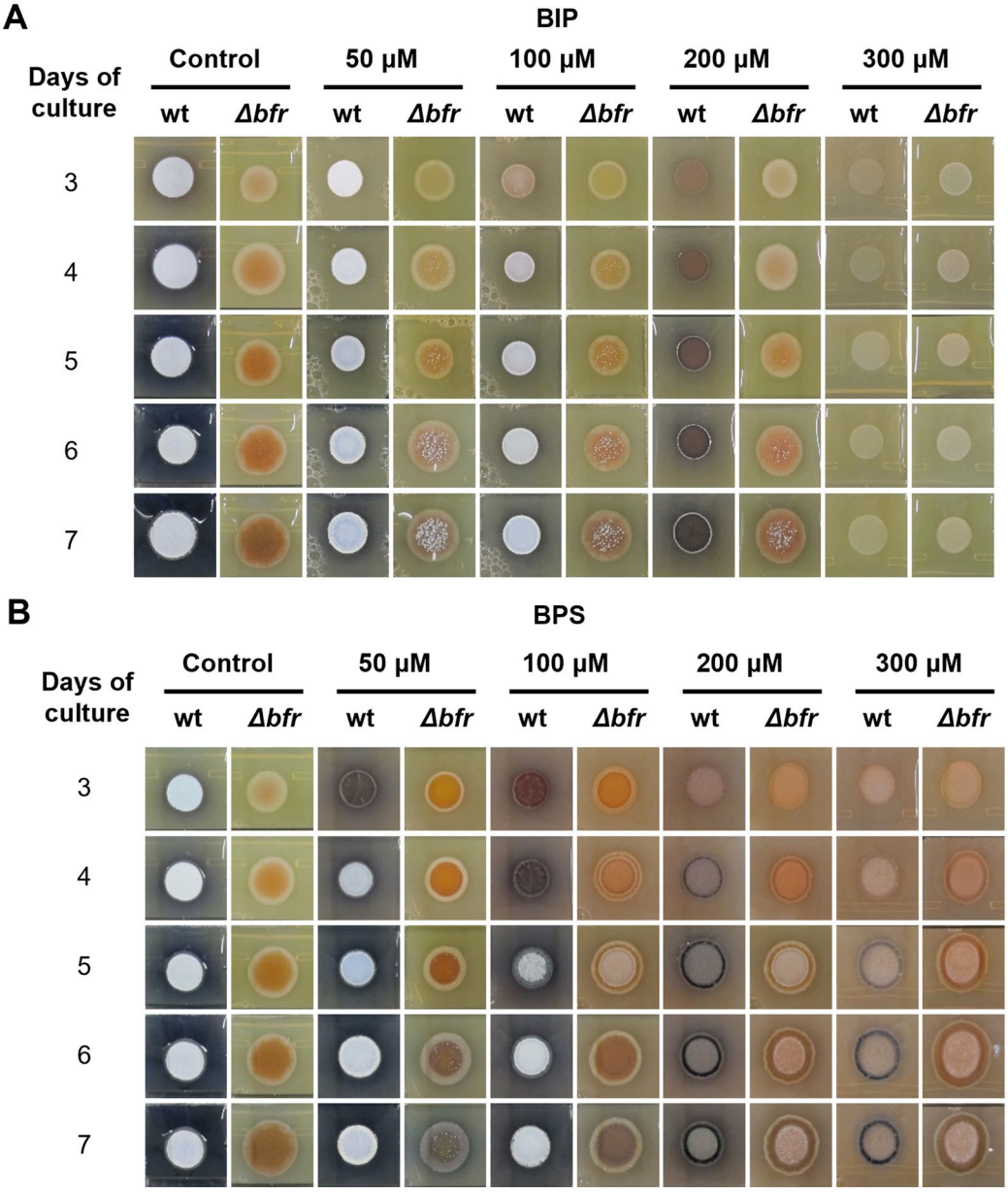

Fig. 5 Effect of iron chelators on differentiation and antibiotic production in *S. coelicolor* M145 and Δ *bfr*. The phenotype of colonies (5×10^5 spores) of M145 and Δ*bfr* on LB supplemented with increasing concentrations (0, 50, 100, 200, and 300 µM) of BIP (**A**) and BPS (**B**) on different days

of the concentrations tested, the phenotype was quite similar: red colonies without aerial mycelium.

This experiment demonstrated that, on LB medium, the chelation of both intracellular and extracellular iron by BIP affects antibiotic production and differentiation in both the wild type and *Δbfr* mutant, while the chelation of extracellular iron by BPS primarily affects aerial mycelium formation with no major changes in the mutant.

Role of bacterioferritin in oxidative stress

The absence of bacterioferritin in the cell could also lead to a compromise in oxidative stress tolerance, as has been observed previously in other microorganisms [71, 72]. Therefore, a survival assay was conducted by treating the spores of both strains with various concentrations of H_2O_2 (0, 4, 8, and 20 mM) and counting the colony forming units (CFUs) formed on YEPD medium. Surprisingly, the *Δbfr* strain had a better survival rate than the wild type after treatment with 4and 8 mM H_2O_2 (Fig. 6A). Indeed, 2–3 CFUs could be observed on plates inoculated with *Δbfr* spores treated with 20 mM H_2O_2, whereas at this concentration, M145 could not survive (Fig. 6A).

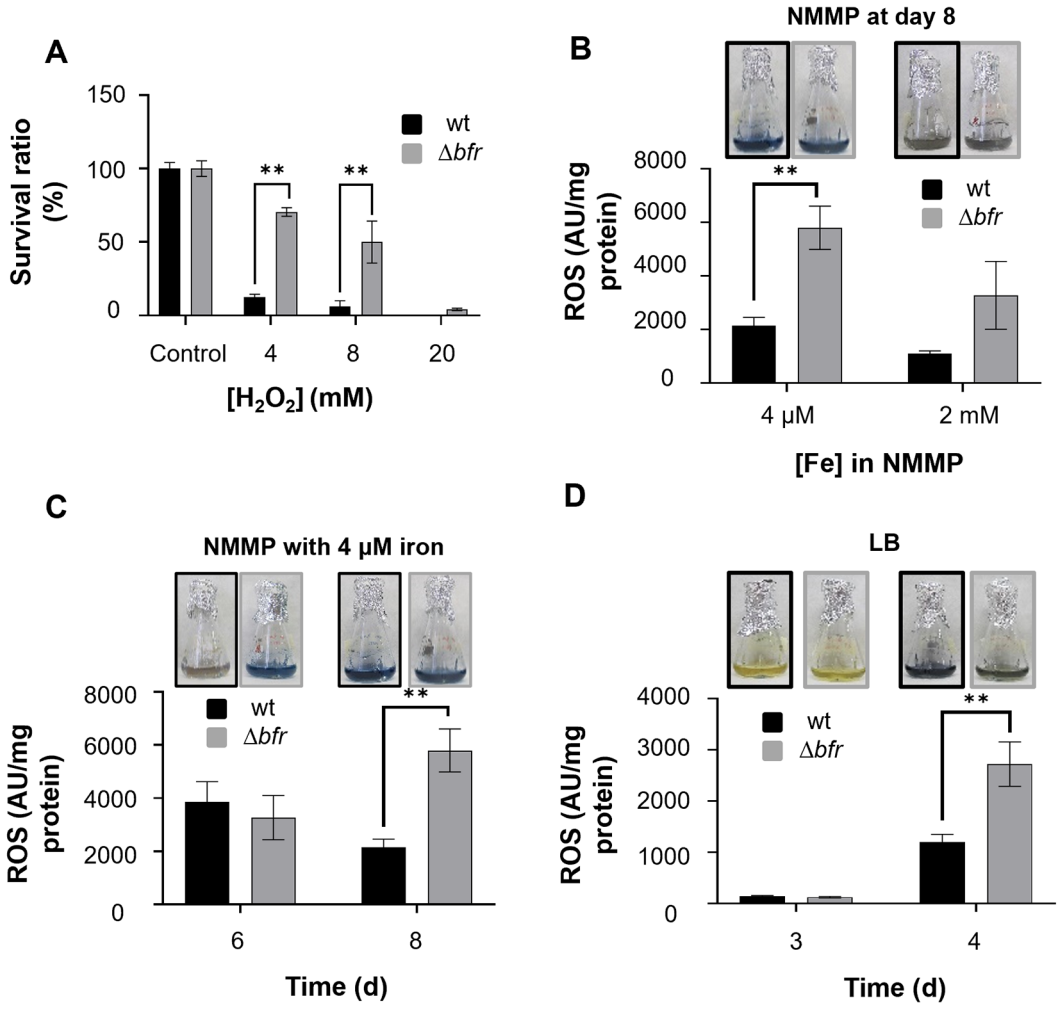

Fig. 6 Role of *bfr* gene in oxidative stress. (**A**) The survival rate of *S. coelicolor* M145 (wt) and Δ*bfr* after treatment with H_2O_2, calculated as the ratio of colony forming units (CFUs) per the number of untreated cells. (**B**) ROS measurement in NMMP with 4 μM and 2 mM iron at day 8. (**C**) ROS measurement in NMMP with 4 μM iron at days 6 and 8. (**D**) ROS measurement in LB at different days. ROS measurements are in AU/mg protein and the phenotypes of the cultures are shown in the upper part of the graphs. Error bars show the standard error of the mean of the experiments carried out in quadruplicate. Asterisks show statistical differences: *: $p < 0.05$; **: $p < 0.01$ (two-way ANOVA)

Bfr influence reactive oxygen species concentration in *S. coelicolor* M145

As previously mentioned and contrary to expectations, *S. coelicolor Δbfr* demonstrated greater tolerance to oxidative stress, with its intracellular iron levels being akin to those of the wild type. The increased tolerance of *Δbfr* to H_2O_2 indicated this protein may be associated with oxidative stress. Furthermore, the link between antibiotic production and oxidative stress had been studied before in *S. coelicolor* [76]. Our hypothesis was that the phenotypic differences observed between the M145 and *Δbfr* strains might be related to reactive oxygen species (ROS) production.

To test this hypothesis, ROS production was measured by using 10 μM $DCFH_2$-DA in both strains grown in liquid NMMP with 10 nM, 4 μM, and 2 mM iron. ROS were quantified at the final time point (8 d) for all three media, although ROS concentration could not be measured in NMMP with 10 nM iron (Fig. 6B). Quantification was also performed on day 6 in NMMP with 4 μM iron (Fig. 6C) when *Δbfr* accelerated ACT production (Fig. 3A).

The results showed that in NMMP with 4 μM iron, ROS concentration was similar in both strains on day 6 (when *Δbfr* accelerates ACT production), but at 8 days, when both strains exhibit similar ACT production, it decreased in M145 and significantly increased in *Δbfr* (Fig. 6C). ROS concentration in *Δbfr* was also higher than in the wild type in NMMP with 2 mM iron on day 8 when both strains produce ACT, but M145 produces more antibiotic (Fig. 6B).

ROS production was also measured in LB medium, on day 3, when both strains have similar ACT production, and on day 4, when ACT synthetized by M145 is greater than in *Δbfr*. As shown in Fig. 6D, ROS concentration was similar on day 3, but higher in *Δbfr* on day 4.

These experiments indicated that the absence of Bfr led to an increase in ROS concentration in *S. coelicolor* which could be related to reduced ACT production.

The deletion of the bacterioferritin gene changes the proteome in *S. coelicolor* M145

As Bfr is not, in principle, a gene expression regulator, the phenotypes observed with the *bfr* gene deletion might be a consequence of changes in *S. coelicolor* metabolism. Therefore, to explore how the absence of Bfr triggers the observed cellular behaviour, a comparative proteomic analysis of the wild type and the Δ*brf* mutant was performed. The assay was conducted on cells obtained from cultures at 3 and 4 days on solid LB medium, where differences between M145 and *Δbfr* were more remarkable (Additional File S8 A). Protein extraction was done as described in the Methods section.

The analysis performed by the Functional Proteomics facility of the Spanish National Centre for Biotechnology (CNB) identified 3521 proteins (approximately 43% of the proteome). The samples showed clear differential clustering for each strain at each culture time using principal component analysis (PCA) (Additional File S9). By setting the threshold to an adjusted p-value < 0.05, 204 proteins were differentially represented in *Δbfr* compared to M145 at 3 days (90 proteins were more abundant in *Δbfr* and 114 proteins were less abundant) and 159 proteins at 4 days (51 proteins were more abundant in *Δbfr* and 108 proteins were less abundant). Additionally, 125 of the differentially represented proteins were detected on both days (Fig. 7A and Additional File S8B).

All differentially represented proteins detected in this study are listed in Additional File S13 (day 3) and Additional File S14 (day 4).

To study how the lack of Bfr could change metabolism, all differentially represented proteins were grouped according to their functions (Fig. 7B). The main results obtained for each functional category are detailed below.

Secondary metabolism

One of the most evident characteristics of the *Δbfr* mutant is a delay in ACT and RED production on LB medium. We detected 15 of the 22 proteins from *act* cluster (*SCO5071-5092*) that were less abundant in *Δbfr* compared to M145. These included proteins responsible for ACT biosynthesis and the regulator ActVI-ORFA (SCO5071) [77]. From the *red* cluster, we only detected four proteins that, contrary to expectations, were more abundant in *Δbfr*: RedS (SCO5585), whose function is unknown, was detected on both days, while three proteins involved in biosynthesis, RedP (SCO5888), RedQ (SCO5887) [78], and RedF (SCO5898) [79] only passed the threshold ($p < 0.05$) on day three (Fig. 8A).

Fourteen proteins from the calcium-dependent antibiotic cluster (CDA) (*SCO3210-SCO3249*), involved in its antibiotic biosynthesis, were more abundant in *Δbfr*. A CDA bioassay confirmed that *Δbfr* produced more CDA than the wild-type strain (Fig. 8B).

Other molecules produced by *S. coelicolor* include yellow coelimycins (yCPKs) P1 and P2 and the antibiotic coelimycin A (abCPK) [80]. Although the ScF (SCO6272) protein, which converts yCPKs to abCPK [50], was more abundant in *Δbfr* than in the wild type, four biosynthetic proteins were less abundant in *Δbfr*. Lower levels of yellow coelimycins were detected in *Δbfr* when both strains were grown on NA medium supplemented with glutamate (Fig. 8C).

Proteins involved in the synthesis of other secondary metabolites also showed changes in abundance. Nine proteins from the cryptic deoxysugar cluster (*SCO0381-SCO0401*), homologous to the *ste* cluster found in *Streptomyces* sp. 139 and thought to be involved in the biosynthesis of ebosin (an exopolysaccharide) [81, 82] were less abundant in *Δbfr*. Other less abundant proteins in the mutant included EctC (SCO1866), involved in the biosynthesis of ectoine, which is implicated in osmotic stress [83], and geosmin synthase (SCO6073) [84]. However, ScbB (SCO6264), involved in γ-butirolactones synthesis [85], was more abundant in the mutant (Additional Files S13 and S14).

Proteins involved in antibiotic regulation

bfr is a direct target of the response regulator AbrC3, which activates antibiotic production [33] and alters its expression in mutants lacking other components of regulatory TCSs related to antibiotic production [32, 34]. Therefore, we also examined which proteins involved in antibiotic regulation altered their abundance in the *Δbfr* mutant.

The *ecr* (*expression coordinated with red*) cluster (*SCO2517-2519*) includes a TCS (EcrA2/SCO2518 and EcrA1/SCO2517) that activates RED [86], and EcrB (SCO2519), a paralogue of the ACT efflux pump ActB/ActII-ORF3 (SCO5084) [87]. Two of these three proteins were detected in higher abundance in the mutant: EcrA2, the HK of the system, and EcrB (Fig. 9A), which is consistent with the higher abundance of some of the proteins from the *red* cluster in the mutant.

Another HK more abundant in the mutant is MtrB (SCO3012) (Fig. 9A). The MtrA-MtrB-LpqB system [88] activates the RR MtrA, which in turn activates aerial mycelium formation [89] and represses antibiotic production regulators [90].

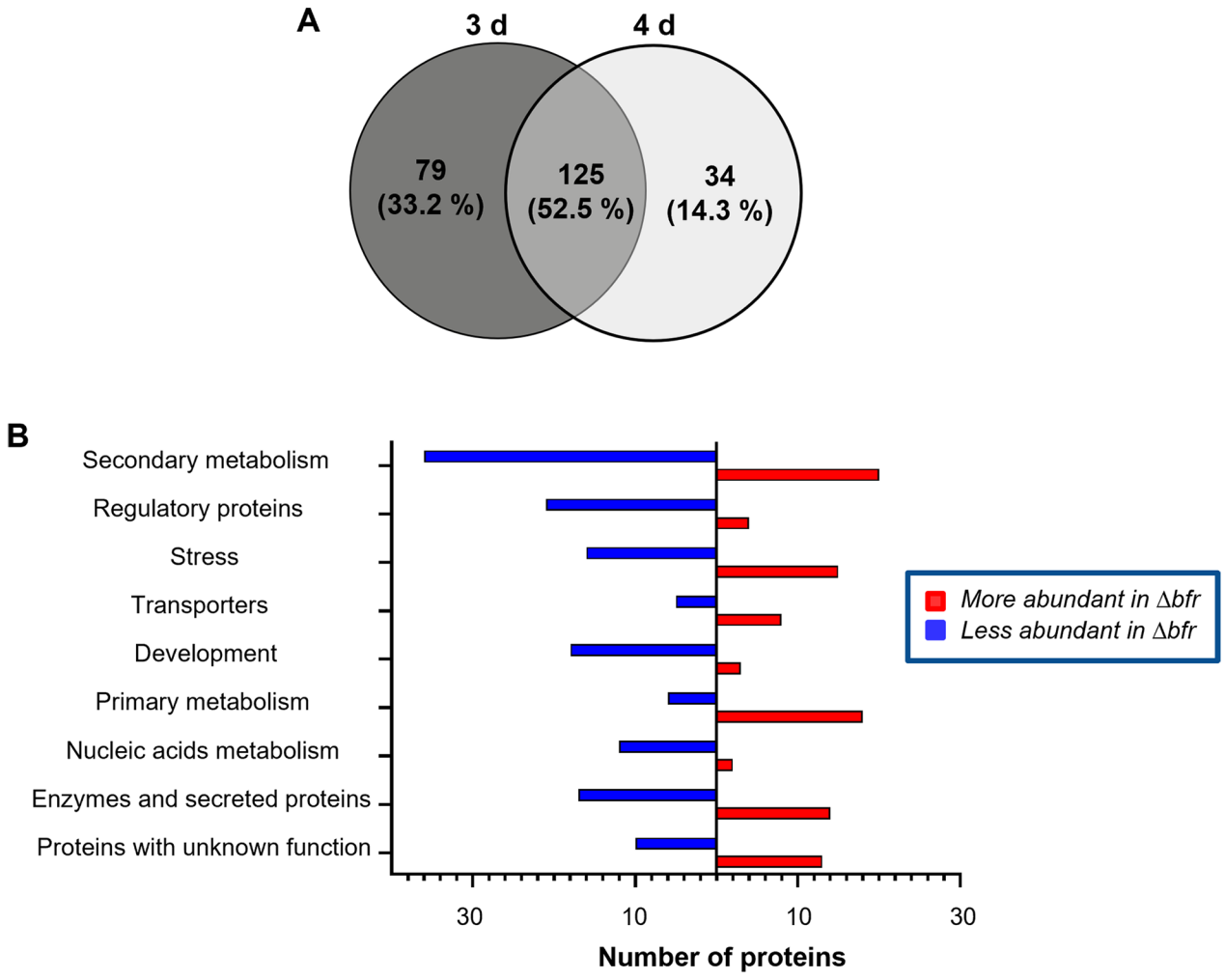

Fig. 7 Proteomic study of *S. coelicolor* Δ *bfr versus* M145 on LB medium. (**A**) Venn diagram showing the total number of differentially represented identified proteins between the wild-type and mutant strains at days 3 and 4 of growth culture (adjusted p-value < 0.05). (**B**) Graphical summary of the number of proteins identified (with adjusted p-value < 0.05) grouped according to their assigned or predicted function

The *abe* (*antibiotic enhancement upon overexpression*) cluster (*SCO3287-3290*) comprises four genes that may function as a signalling transduction system and enhancers of ACT production [91]. Three proteins from this cluster had lower abundance in the *Δbfr* mutant: AbeB (SCO3288) and AbeC (SCO3289) are membrane proteins, and AbeD (SCO3290) has a cyclic nucleotide-binding domain (Fig. 9A).

The role of XRE/DUF397 proteins in antibiotic production in *S. coelicolor* has recently been studied [92]. In our analysis, three XRE proteins, SCO4678, SCO5125, and SCO6629 were less abundant in the *Δbfr* mutant (Fig. 9A).

Additionally, two regulatory proteins were less abundant in the *Δbfr* mutant: NsdB (SCO7252) and EshA (SCO7699). NsdB (*negatively affecting Streptomyces physiological differentiation*) represses antibiotic production in some culture media [93], and EshA is required to keep ppGpp levels high enough to enhance ACT production and aerial mycelium in certain culture media [94] (Fig. 9A).

The *Δbfr* mutant also exhibited changes in proteins from uncharacterised TCSs that could regulate antibiotic production or other processes (see Additional Files S13 and S14). Moreover, several proteins from the so-called "conservons" have been assigned regulatory roles, as explained below.

Conservons

cvn operons are gene clusters with a conserved structure. These genes encode proteins that could function as eukaryotic G signalling proteins: a histidine kinase-like protein (CvnA), two hypothetical proteins (CvnB and CvnC), and an ATP or GTP-binding protein (CvnD). *S.*

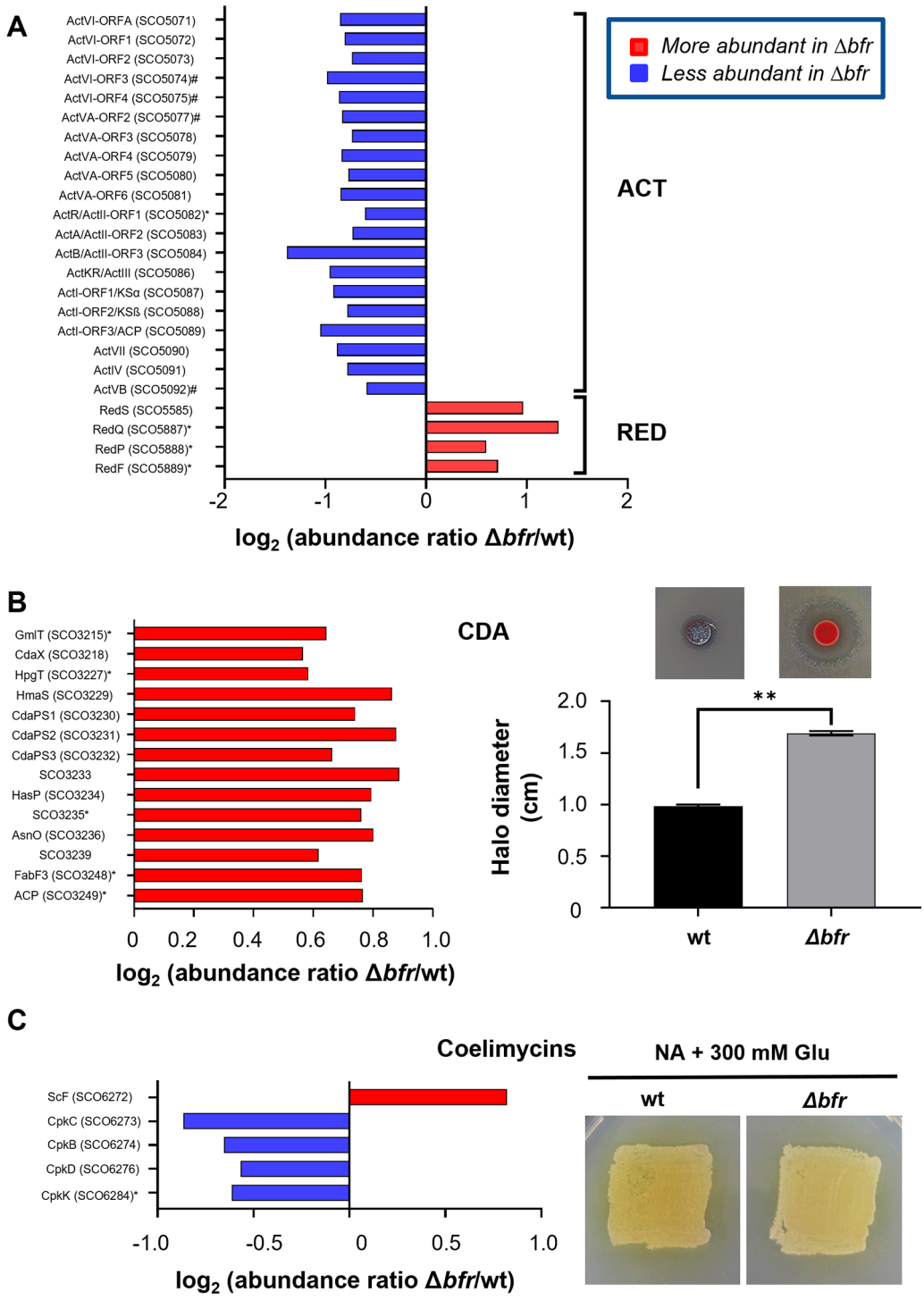

Fig. 8 Proteins linked to secondary metabolism detected in the proteomic study. Proteins marked with * were only detected at day 3, and those marked with # were only detected at day 4. Represented ratios are the mean for proteins detected at both days. (**A**) Abundance ratios of proteins from *act* and *red* cluster. (**B**) Abundance ratios of proteins from *cda* cluster and CDA production assay (measurement of inhibition halos against *B. subtilis*). Error bars show the standard error of the mean of the experiments carried out in triplicate. Asterisks in the graph show statistical differences between the two strains: *: $p < 0.05$; **: $p < 0.01$ (t-test). (**C**) Abundance ratios of proteins from *cpk* cluster and yCPKs production assay

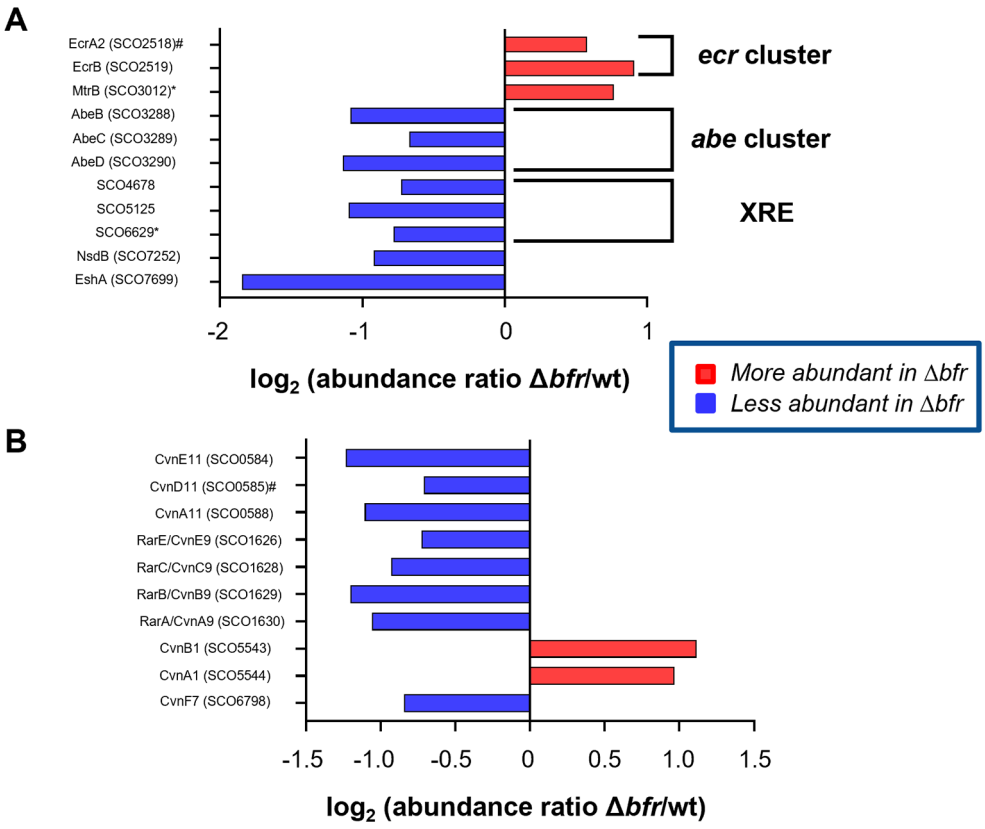

Fig. 9 Proteins linked to secondary metabolism regulation detected in the proteomic study. Proteins marked with * were only detected at day 3, and those marked with # were only detected at day 4. Represented ratios are the mean for proteins detected at both days. (**A**) Abundance ratios of other proteins which regulate secondary metabolism. (**B**) Abundance ratios of proteins from conservons

coelicolor possesses 13 conservons, four of which include an additional gene encoding a cytochrome P450 protein (CvnE) [95].

From the first conservon, *cvn1* (*SCO5541-SCO5544*), CvnA1 (SCO5544), and CvnB1 (SCO5543) were more abundant in the *Δbfr* mutant. This conservon is involved in the coordination between glucose concentrations and development by regulating the sigma factor SigU, which represses differentiation and antibiotic production [96] (Fig. 9B).

The *cvn7* operon is involved in the interaction of *S. coelicolor* with other microorganisms. This cluster includes an additional gene, *cvnF7* (*SCO6798*), which encodes a cyclic nucleotide-binding protein, and it is homologous to *cvnF8* (*sco6939*), which is involved in secondary metabolism and cryptic cluster regulation [97]. CvnF7 was less abundant in the *Δbfr* mutant (Fig. 9B).

The *cvn9* operon (*SCO1626-1630*), also known as *rar* (*restoration of aerial mycelium in* amf*R mutant*), encodes proteins characterized as repressors of differentiation and secondary metabolism under normal conditions [95]. RarA/CvnA9 (SCO1630), RarB/CvnB9 (SCO1629), RarC/CvnC9 (SCO1628), and RarE/CvnE9 (SCO1626) were less abundant in the *Δbfr* mutant compared to the wild type (Fig. 9B).

Finally, three proteins from an uncharacterised conservon, *cvn11* (*SCO0584-0588*), were also less abundant in the *Δbfr* mutant: CvnA11 (SCO0588), CvnD11 (SCO0585, only detected on day 4), and CvnE11 (SCO0584) (Fig. 9B). CvnA11 has been described as a modulatory protein for several genes [98] and a regulator of nitrogen metabolism [99].

Oxidative stress and respiration

As mentioned earlier, the *Δbfr* mutant demonstrated better tolerance to oxidative stress (Fig. 6A) and had a higher intracellular ROS concentration (Fig. 6B, C and D). Consequently, proteins involved in oxidative stress were analysed to determine the presence of a stress response or a related pathway highly represented in the mutant.

Since the levels of ACT biosynthetic proteins were lower in the mutant on LB, resulting in reduced ACT production, the response to redox metabolites, such as ACT and its precursors, was also diminished in the mutant. SoxR (SCO1697) activates the expression of five genes in response to ACT or its derivatives to protect

against side effects [100, 101]. Four of the five proteins encoded by these genes were less abundant in the mutant on day 3 (Additional File S10A): EcaA (SCO7008), an ABC transporter; EcaB (SCO1909), a monooxygenase which could modify ACT; EcaD (SCO4266), an NADPH-dependent quinone reductase positively regulated by ActVI-ORFA (also less abundant in *Δbfr*, see "Secondary metabolism" section) [77]; and SCO2478, an NADPH-dependent flavin reductase.

Furthermore, all detected proteins related to oxidative respiration were more abundant in *Δbfr* (Additional File S10B): *bcc-aa*$_3$ supercomplex subunits QcrB (SCO2148), CtaE (SCO2151) and CtaC (SCO2156) [102]; the cytochrome maturation protein ResA (SCO4472); respiratory chain complex I subunits NuoH (SCO4569), NuoL (SCO4573) and NuoM (SCO4574); and ATPase subunits AtpI (SCO5366), AtpB (SCO5367) and AtpE (SCO5368) [76, 103]. Moreover, GabD (SCO7035), a succinate-aldehyde dehydrogenase linked to NADH production in *S. coelicolor* [76], was also more abundant in the mutant. This could result in higher O_2 consumption, promoting the faster growth observed in the *Δbfr* mutant and early hypoxia.

In this context, it is known that the two-component system OsdK/DevS-OsdR/DevR (SCO0203-0204) activates a dormancy response under hypoxic conditions [104]. Two proteins activated by OsdR were more abundant in the *Δbfr* mutant (Additional File S10 A): SCO2367, a secreted serine peptidase [104], and SCO6164, a paralogous of DksA from *E. coli* [105], a transcription factor which modulates RNA polymerase by ppGpp levels [106, 107] (Additional File S10 A).

Tdd8 (SCO2368) is a protein involved in calcium homeostasis that represses genes involved in oxidative stress response and dormancy [108]. Although Tdd8 was not detected in our analysis, some proteins repressed (directly or indirectly) by Tdd8 were more abundant in the mutant compared to the wild type (Additional File S10 A). Two of these proteins repressed by Tdd8 are involved in nitrogen metabolism and are positively regulated by OsdR. These proteins are NarG2 (SCO0216) and NarI2 (SCO0219), the catalytic and the γ subunits, respectively, of the nitrate reductase Nar2, the main nitrate reductase of *S. coelicolor*, [109]. By contrast, NarH1 (SCO6534), the catalytic subunit of Nar1, was detected on both days but was less abundant in the mutant. Nar1 is the nitrate reductase which reduces nitrate in spores [110]. Endogenous nitric oxide in *S. coelicolor* has been linked to RED and ACT production, under certain levels, and a delay in differentiation [111, 112].

Another two proteins repressed by Tdd8 and overrepresented in the proteomic assay were SCO168 (a cyclic nucleotide-binding protein from family CRP/FNR) and SCO0169 (a putative cystathionine β-synthase) [108]. These proteins are related to oxidative and nitrosative stress protection because cystathionine is an intermediate in cysteine biosynthesis, which is a precursor of mycothiol, involved in these types of stress [113, 114]. Moreover, another protein, SCO2763, linked to mycothiol, was detected on day 3 and was more abundant in the mutant. SCO2763 is an ABC transporter activated by SigR in oxidative stress from thiol groups, transporting mycothiol conjugates [115].

Two more proteins directly related to oxidative stress were detected on both days (Additional File S10A). MetQ (SCO1557), a lipoprotein more abundant in the *Δbfr* mutant than in the wild type, is involved in methionine import together with MetI and MetN. The three genes encoding these proteins are overexpressed in oxidative stress [24]. Conversely, AhpC (SCO5032) was less abundant in the mutant. This protein is an alkyl hydroperoxide reductase induced by OxyR in oxidative stress, acting in defence against endogenous hydrogen peroxide [116].

Regarding other proteins less abundant in *Δbfr* compared to the wild type, we found two membrane proteins with thioredoxin domains (Additional File S10A); thioredoxins are involved in various oxidative stress responses. These proteins are SCO2035, which has been described as more abundant in multinucleated mycelia [117], and SCO2989 which has not been studied and only surpasses the $p<0.05$ threshold on day 3.

Cellular envelope stress and transporters

The cellular envelope is another significant source of stress. The ECF sigma factor SigE controls the expression of genes that encode membrane proteins in response to this stress [118]. Three proteins whose genes are regulated by SigE were more abundant in the mutant: SCO4134, a putative oxidoreductase similar to *Pseudomonas putida* 4-cresol dehydrogenase, SCO4471, a lipoprotein involved in antibiotic and lysozyme resistance, and SCO5213, a metallopeptidase [118] (Additional File S11A).

Two proteins from an ABC transporter associated with stress from antibiotics affecting the cell wall were less abundant in the *Δbfr* mutant: SCO3110 (only detected on day 4) and SCO3111 [119] (Additional File S11A).

Many membrane proteins with transport functions (predicted or described) had altered abundance levels in *Δbfr* (Additional File S11A). Two transporters were more abundant in the mutant and were detected on both days: SCO1655, an oligopeptide transporter [120], and KdpB (SCO3717), a subunit of a potassium importer [121]. On day 3, a putative metal and/or siderophore transporter, SCO0996 [122], was less abundant in the mutant.

Osmotic stress

As mentioned in the "Secondary metabolism" section, one of the proteins required for ectoine production in osmotic stress (EctC/SCO1866) [83] was less abundant in *Δbfr*, similar to DpsA, which is known to play a role in osmotic stress [21, 123] (Additional File S11B). Osmotic stress in *S. coelicolor* is mainly regulated by SigB [124]. SigB was not detected in this proteomics analysis, but its anti-sigma factor, RsbA (SCO0599), which releases SigB in osmotic stress [125], was less abundant in the mutant. This could indicate that SigB is more active in *Δbfr* than in the wild type, but we did not observe an active osmotic stress response. The abundance of proteins regulated by SigB was variable: SCO3343, a protein with a GsmA (*sporangiosporematuration cell wall hydrolase*) domain [126], and SCO6014, a putative amino acids transporter [127], were more abundant in the mutant, while SCO5207, a putative regulatory protein from cystathionine beta-synthase family [126], was less abundant.

Another protein with a role in osmotic stress, SmpA (SCO2529), was less abundant in the *Δbfr* mutant (Additional File S11B). SmpA is a metalloprotease that activates the catalase CatB, required for osmotic protection and differentiation [128].

Differentiation and development

Another important phenotype shown by the *Δbfr* mutant was delayed differentiation on LB (Fig. 1). In this way and as expected, some proteins involved in *Streptomyces* development were less abundant in *Δbfr* (Fig. 10). As Table 1 shows, these proteins were: DpsA (SCO0596), SCO1756, RpfC (SCO3098), BldN (SCO3323), RsbN (SCO3324), BdtA (SCO3328), RsfA (SCO4677), BldM/WhiK (SCO4768), SCO4920, SCO5029, EshB (SCO5249), FilP (SCO5396), BldB (SCO5723), WhiH (SCO5819), and CabC (SCO7647).

Regarding proteins more abundant in the *Δbfr* mutant compared to the wild type, we only detected Cis1 (SCO4242) on day 4, which is involved in programmed cell death [134] (Fig. 10).

Primary metabolism

Proteins from glycolysis and the Krebs cycle were not detected in the proteomics study. Four proteins related to carbohydrate transport and degradation were more abundant in *Δbfr* (Additional File S12A): XylF (SCO6009) and BxlE1 (SCO7028), which are involved in the binding and import of xylose [142] and xylobiose [143], respectively, and CsnB (SCO2024) and DagB (SCO3487), a chitosanase [144] and an agarase [145], respectively.

AccB (SCO5535), an essential component from acetyl-CoA carboxylase that produces malonyl-CoA for fatty acids biosynthesis [146], was less abundant in *Δbfr* (Additional File S12A). FabH (SCO2388), a β-ketoacyl ACP synthase involved in fatty acids biosynthesis [147], was also less abundant in the mutant but was only detected

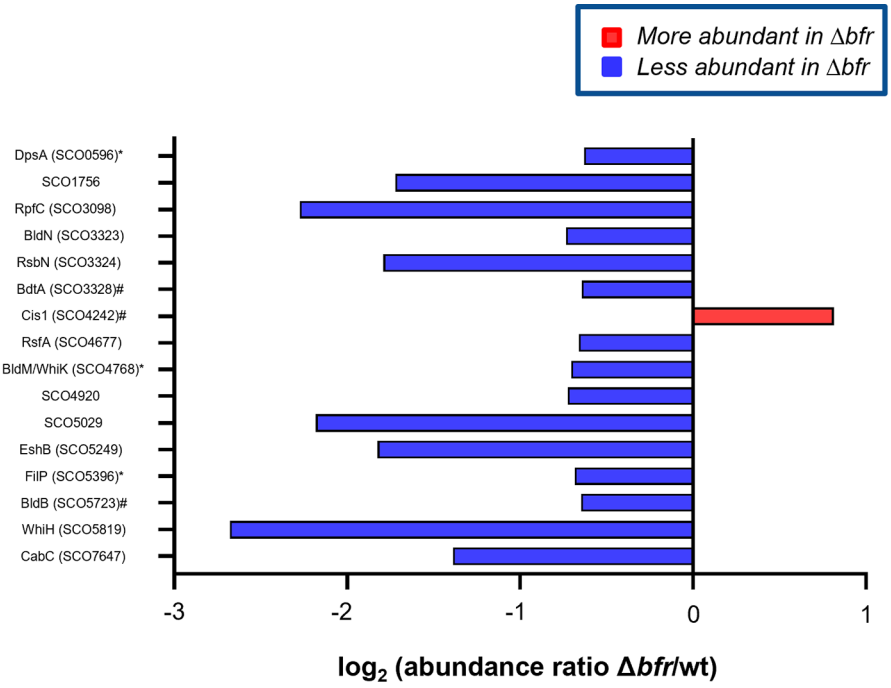

Fig. 10 Proteins linked to development detected in the proteomic study of *S. coelicolor* Δ *bfr versus* M145. Abundance ratios of proteins. Proteins marked with * were only detected at day 3, and those marked with # were only detected at day 4. Represented ratios are the mean for proteins detected at both days

Table 1 Proteins linked to development detected in the proteomics study of *S. Coelicolor Δbfr versus* M145

Protein Name (SCO)	Function	Outcome	Reference
DpsA [a] (SCO0596)*	Dps protein	nucleoid condensation in sporulation	[21]
SCO1756 [a]	uncharacterized protein	might be involved in differentiation	[129]
RpfC [a] (SCO3098)	*r*esuscitation-*p*romoting *f*actor (Rpf)	breaks cellular walls in germination	[130]
BldN [a] (SCO3323)	extracytoplasmic function (ECF) sigma factor	controls the expression of chaplins and rodlins	[131, 132]
RsbN [a] (SCO3324)	anti-sigma factor	represses BldN	[131]
BdtA [a] (SCO3328)#	putative transcription factor	might be involved in differentiation	[133]
Cis1 [b] (SCO4242)	contractile injection system	programmed cell death (PCD)	[134]
RsfA [a] (SCO4677)	anti-sigma factor	inhibits SigF (sporulation) and BldG (osmotic stress)	[135, 136]
BldM/WhiK[a] (SCO4768)	transcription factor	involved in aerial mycelium formation, activated by BldN	[132, 133]
SCO4920 [a]	orthologous to SdrA of *S. avermitilis*	involved in sporulation	[137]
SCO5029 [a]	related to Rpf	-	[130, 138]
EshB [a] (SCO5249)	cyclic nucleotide-binding protein	involved in sporulation	[139]
FilP [a] (SCO5396)*	cytoskeletal protein	growth	[140]
BldB [a] (SCO5723)#	regulatory protein	controls sporulation	[141]

[a] Proteins that were less represented in the mutant strain. [b] Proteins overrepresented in the mutant. Proteins marked with * and # were only detected at days 3 and 4, respectively

above the threshold ($p<0.05$) on day 4. Two proteins related to cholesterol metabolism were more abundant in *Δbfr*: SCO4781 (only detected on day 4), homologous to *Mycobacterium tuberculosis* ChoD (cholesterol oxidase) [148], and SCO5420, a putative cholesterol esterase that can degrade detergents to use them as carbon source [149].

Two proteins involved in amino acids biosynthesis were less abundant in the mutant (Additional File S12A): SerA (SCO5515, only detected on day 3), for serine biosynthesis [150], and ArgG (SCO7036), for arginine biosynthesis [151].

Ribosome and DNA

Eight ribosomal proteins, seven from 30 S subunit (RpsD/SCO1505, RpsT/SCO2563, RpsR1/SCO3908, RpsL/SCO4659, RpsN1/SCO4715, RpsI/SCO4735, and RpsP/SCO5591) and one from 50 S subunit (RpmB1/SCO5564), were less abundant in the mutant (Additional File S12B). This suggests that *Δbfr* could be less efficient during translation.

A few proteins related to DNA processing were also detected (Additional File S12B). AdnA (SCO5183), involved in DNA recombination [152], was one of the most abundant proteins in the *Δbfr* mutant. Another protein more abundant in *Δbfr* was SCO3619, which belongs to YbaB/EbfC family of nucleoid-associated proteins and could have a role in DNA repair [153].

Finally, LexA (SCO5803), which represses the SOS response under normal conditions [154], was less abundant in the mutant on day 3 (Additional File S12B).

Discussion

Iron as a signal in antibiotic biosynthesis and development in *S. coelicolor M145*

Antibiotic regulation in *Streptomyces* is a complex network of regulatory proteins linked to environmental signals [4]. Iron is one of these key signals, and the relationship of iron, proteins related to iron metabolism, and secondary metabolism in *Streptomyces* has been well-documented [5, 6, 29, 74, 155]. Previous studies on *S. coelicolor*'s TCSs, which play a major role in cellular signalling, have validated the relationship between these regulatory systems and the *bfr* gene, which encodes for a bacterioferritin [34, 35, 155]. In other actinomycetes, the link between iron homeostasis and secondary metabolism has also been described, as in *S. avermitillis*, where the DtxR-family regulator IdeR is required for the proper production of avermectins and activates, among other genes, the expression of *bfrA* to store excess iron [30]. On the other hand, Bfr from *Saccharopolyspora pogona* plays a role in iron storage and oxidative stress tolerance, and enhances butenyl-spinosyn production [71].

In our study, the absence of the bacterioferritin in *S. coelicolor* caused a delay in differentiation and antibiotic production on complex media (Figs. 1 and 2). In the minimal medium NMMP, where iron concentrations can be controlled, ACT and RED production differed between liquid and solid media. Lee et al. reported that low iron conditions increased ACT production on CYE medium [74]. In our study, low iron conditions in solid NMMP enhanced antibiotic production (Fig. 3B), while high iron concentrations inhibited development on solid medium and the production of both antibiotics. However, in liquid NMMP with high iron concentrations, cultures of the wild-type strain M145 enhanced ACT and RED production but not the mutant (Fig. 3A). Liquid non-sporulating cultures exhibit greater expression of genes linked to oxidative stress, among others [156], so antibiotic production in liquid cultures could be linked to increased stress and, possibly, to the differential expression of some regulatory genes.

Growth assays in the presence of the iron chelators BIP and BPS demonstrated that both extracellular and intracellular iron play a role in *S. coelicolor* wild-type development and antibiotic production (Fig. 5). The lack of significant changes in the *Δbfr* mutant, regardless of the presence of the chelator, could be attributed to a possible role of Bfr as an iron donor for regulatory proteins containing Fe-S clusters (Fig. 11). Since the absence of Bfr negatively affected the iron levels required for regulatory proteins, they would remain inactive whether iron was chelated or not (see below).

The presence of only one bacterioferritin in *S. coelicolor M145* and its role in iron storage

While in *S. coelicolor* the bacterioferritin Bfr, the subject of this study, is the only putative canonical iron storage protein, other bacteria, such as *E. coli*, *Campylobacter jejuni*, *Pseudomonas aeruginosa*, and *M. tuberculosis*, possess two types of these proteins, bacterioferritin and ferritin, each with a specific role in each organism. In *M. tuberculosis*, which belongs to the phylum *Actinomycetota*, like *Streptomyces*, there is one bacterioferritin (BfrA), RV1876, which is 62% identical to the one studied in this work, and one ferritin (Ftn, previously named "BfrB"), RV3841, which does not have a homologue in *S. coelicolor*. Both proteins protect *M. tuberculosis* from oxidative stress. However, Ftn has a stronger iron storage capacity and plays a role in higher iron concentrations. By contrast, BfrA acts under low iron conditions to maintain basal iron levels. Only the expression of Ftn is induced with iron by IdeR, the homologue of DmdR1 in *Mycobacterium* [16]. Interestingly, in *Mycobacterium abscessus* subsp. *massiliense*, an emerging pathogen that causes non-tuberculosis diseases, two genes for ferritins have been described, although there are no genes present for bacterioferritin [157]. In *P. aeruginosa*, the bacterioferritin (BfrB) that coexists with a ferritin (FtnA, previously named "BfrA") is responsible for iron accumulation and requires specific interaction with a bacterioferritin-associated ferredoxin (Bfd) to mobilise iron. In *P. aeruginosa*, FtnA seems to provide iron to the catalase KatA [27]. The interaction with Bfd also occurs in *Erwinia chrysanthemi* [158]. Therefore, there are specific roles for each type in each microorganism; for example, in *E. coli* the most important ferritin is FtnA [27].

The deletion of iron storage proteins in other microorganisms or the disruption of iron release from these proteins changes intracellular iron concentrations [27]. In *P. aeruginosa*, the lack of BfrB (the main iron storage protein) reduces total iron levels, prompting the cell to decrease iron uptake. Conversely, inhibiting the BfrB-Bfd interaction results in an irreversible flux of iron towards BfrB, thereby decreasing the labile iron concentration [27]. However, in our study, which tested NMMP with three different iron concentrations and LB, there were no differences in total and labile iron concentrations between the *Δbfr* mutant of *S. coelicolor* and the M145 strain (Fig. 4).

Regarding the putative transcriptional regulation of bacterioferritins, the promoter region of *bfrA* from *S. avermitilis* contains iron boxes (GCAGGACACGGAT CGTCATA) and is activated by IdeR, the homologue of DmdR1 and DmdR2 from *S. coelicolor* [30]. However, no iron boxes have been detected in the promoter of the *bfr* gene of *S. coelicolor* [159]. The absence of these boxes in the *S. coelicolor bfr* promoter and the lack of differences in iron concentrations between M145 and *Δbfr* mutant could indicate that, in *S. coelicolor*, Bfr might have other functions beyond iron storage. Dps proteins (DpsA, DpsB, and DpsC in *S. coelicolor*), which also possess iron storage capacity [23], could be compensating (among others) for the lack of Bfr, as described in other organisms [158] (Fig. 11B).

The role of bacterioferritin in *S. coelicolor* M145 in oxidative stress and iron loading to regulatory proteins

The absence of iron storage proteins in other organisms causes susceptibility to oxidative stress since ROS derived from the Fenton reaction cause damage to cellular structures (71, 72). Here, we report the contrary response from *S. coelicolor* M145: the *Δbfr* mutant shows increased tolerance to oxidative stress (Fig. 6A), even when intracellular ROS concentration is higher in the mutant in both complex (LB medium, Fig. 6D) and minimal (NMMP, Fig. 6B and C) media.

These results lead us to consider that Bfr from *S. coelicolor* could act as a modulator of oxidative stress, storing iron inside its cavity to prevent Fenton reaction and maintaining normal oxidative stress levels. In this way, Bfr from *Desulfovibrio vulgaris* acts as a protective system against ROS and is activated by the oxidative stress regulator PerR, while Ftn does not play a role in ROS protection [160]. Moreover, like Ftn from *P. aeruginosa*, which provides iron to another protein [27, 161], Bfr from *S. coelicolor* could play a similar role. Parallel functions have been linked to other ferritins: in *E. coli*, FtnA can store iron from damaged Fe-S clusters and this iron is transferred to the protein IscA (with the thioredoxin reductase system), which transfers it to the scaffold protein IscU from the Isc system, for Fe-S biosynthesis [162]. In *E. chrysanthemi*, iron from siderophores is captured by the Suf system, which synthesises Fe-S clusters and incorporates this iron into Bfr [158]. One of the ferritins of *Salmonella enterica* sv. *Typhimurium*, FtnB, can use stored iron to repair damaged Fe-S clusters [163]. Thus, in *S. coelicolor*, Bfr could be transferring iron to regulatory proteins involved in differentiation, antibiotic production, and other processes (Fig. 11A). Several

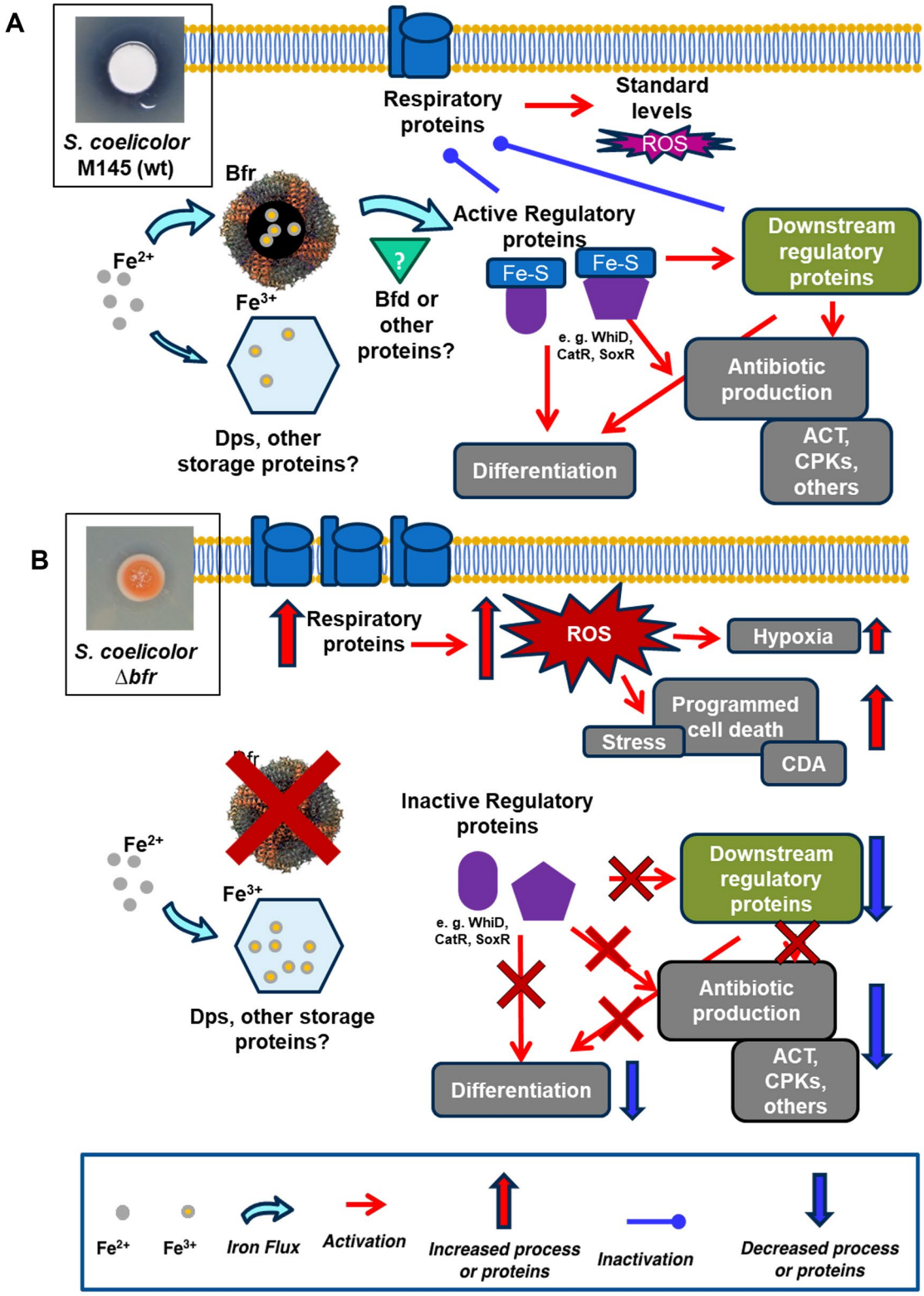

Fig. 11 Proposed model of the role of Bfr in *S. coelicolor* M145. (**A**) In the presence of Bfr, proteins with Fe-S clusters can receive iron and participate in the regulation of other proteins. Secondary metabolites (ACT, CPKs, etc.) are produced under normal conditions. ROS are produced at standard levels. (**B**) In the absence of Bfr, regulatory proteins with Fe-S clusters do not receive enough iron, so differentiation and secondary metabolism are impaired. More ROS are produced and *S. coelicolor* activates oxidative respiration, growth, programmed cell death (with CDA biosynthesis), hypoxia, and stress responses

regulatory proteins have Fe-S clusters or are iron coupled, like the Wbl family, involved in differentiation [164], and proteins involved in redox sensing and resistance, such as CatR [165], which is also involved in iron homeostasis [166]. The source of iron for Fe-S clusters assembly is still unknown [167, 168]. In *S. coelicolor*, the contiguous gene, *SCO2114*, codes for a putative ferredoxin Bfd, which could help Bfr to reduce stored iron and transfer it to regulatory proteins. According to our proposed role of Bfr, the Fe-S or iron-containing proteins would be inactive in the *Δbfr* mutant, and the proteins regulated by these iron-containing upstream regulators (proteins from conservons, some TCSs, metabolism regulators, secreted proteins, etc.) would change their abundance and produce the phenotype seen in the mutant (Fig. 11B).

On the other hand, oxidative stress related to respiration regulates antibiotic production in *S. coelicolor*, and these antibiotics act as modulators of programmed cell death (RED, CDA) and antioxidants (ACT) [76, 169]. In this context, the accelerated production of ACT in NMMP with 4 µM iron in the *Δbfr* mutant could be produced by higher ROS production, which triggers ACT to neutralise them, leading to concentrations similar to those found in the wild type on day 6. However, as Bfr is absent, the concentrations of ROS continue to increase in the mutant on day 8 (Fig. 6B). In solid NMMP with 2 mM iron, iron could produce an excess of ROS, above a certain threshold, which blocks differentiation and secondary metabolism. By contrast, in liquid NMMP, this iron could be less available, and/or cells are more tolerant to stress due to the greater expression of genes linked to oxidative stress [156], and iron enhances ACT production in M145, but produces too much oxidative stress in *Δbfr* (Fig. 6C).

The proteomics study performed on LB medium, where *Δbfr* mutant also showed higher ROS concentration, did not show a general oxidative stress response enhanced due to the lack of Bfr. Instead, proteins related to hypoxia [104] and activated in oxidative stress [108] (Additional File S10A), oxidative respiration (Additional File S10B), and secondary metabolites (CDA) related to programmed cell death (Fig. 8B) [169] were more abundant (Fig. 11). These mechanisms could be a response to a higher ROS concentration. Thus, the *Δbfr* mutant would try to consume more oxygen, causing a higher growth rate, but also activating dormancy and stress responses. This response could not be enough to permanently decrease ROS concentration, so high ROS levels, and/or the lack of functional iron clusters inside regulatory proteins (as explained before), would be blocking downstream regulatory proteins, differentiation, and some metabolic processes, such as fatty acid biosynthesis and some secondary metabolites production (deoxysugar, coelymicins, etc.). Despite an altered development and the hypothetical absence of these functional regulatory proteins, the cellular response of the mutant would allow it to survive in higher oxidative stress conditions without significant changes in iron concentrations.

ACT production could also be reduced by the absence of SoxR in its active form: SoxR is a [2Fe-2 S] protein [170], which activates proteins for ACT detoxification [100, 101], and these proteins were less abundant in the *Δbfr* mutant on day 3 (Additional File S10 A), which could indicate a decrease in SoxR activity.

These assumptions regarding the role of Bfr in *S. coelicolor* should be further studied by checking whether Bfr can interact with Fe-S clusters containing regulatory proteins or other iron-associated proteins. Additionally, it would be interesting to study the proteomes of *S. coelicolor* M145 and *Δbfr* in minimal media with different iron concentrations, with a special focus on the accelerated production of ACT with 4 µM iron and the differences seen between liquid and solid NMMP with 2 mM iron. The molecular mechanism of the role of Bfr in *S. coelicolor* needs to be further explored to understand the role of iron in *S. coelicolor* metabolism and enhance the production of bioactive metabolites.

Conclusions

The bacterioferritin from *S. coelicolor* plays an important role in antibiotic production and development. Although its function in iron storage appears to be replaceable, Bfr could also have a role modulating reactive oxygen species (ROS) levels and facilitating iron transfer to regulatory proteins. The absence of Bfr significantly impacts the regulation of proteins involved in secondary metabolism and differentiation, among others. Additionally, the influence of iron on antibiotic production varies between solid and liquid minimal media, and Bfr plays a role in this effect.

Therefore, to optimize the production of bioactive molecules and discover new ones, it is essential to consider iron, its storage proteins, and oxidative stress as components of the complex regulatory network of antibiotic production in actinomycetes.

Supplementary Information

The online version contains supplementary material available at https://doi.org/10.1186/s12934-024-02510-1.

Supplementary Material 1: Plasmids used in this work.

Supplementary Material 2: Oligonucleotides used in this work.

Supplementary Material 3: Checking of Δ*bfr* deletion mutant. Scheme of the location of the primers used in the genome of the *S. coelicolor* M145 wild-type strain (top) and the size of the fragments produced by PCR in the wild-type and Δ*bfr* (ΔSCO2113) strains (bottom).

Supplementary Material 4: Overexpression of *bfr*. (A) Comparison of antibiotic production and differentiation of *S. coelicolor* M145 with the empty vector (pN702GEM3) and with pN-Bfr (overexpressing *bfr*) grown on LB, R2YE, and YEPD with neomycin at 3, 7, and 10 days. (B) RED (left) and ACT (right) quantification of liquid cultures in LB with neomycin in µM/mg.

Error bars show the standard error of the mean of the experiments carried out in triplicate. Asterisks show statistical differences between the two strains at each time point: *: $p<0.05$; **: $p<0.01$ (two-way ANOVA).

Supplementary Material 5: *S. coelicolor* phenotype in NMMP liquid. Progression of the production of coloured antibiotics in liquid cultures of *S. coelicolor* M145 (wt) and Δ*bfr* mutant in NMMP with 10 nM, 4 µM, and 2 mM iron for 10 days.

Supplementary Material 6: Antibiotic quantification in liquid NMMP. ACT (A) and RED (B) quantified from liquid cultures of S. coelicolor M145 (wt) and Δ*bfr* mutant in NMMP with 10 nM (top), 4 µM (center), and 2 mM (bottom) iron for 8 days. Error bars show the standard error of the mean of the experiments carried out in quadruplicate. Asterisks show statistical differences between the two strains at each time point: *: $p<0.05$; **: $p<0.01$ (two-way ANOVA).

Supplementary Material 7: Effect of iron on antibiotic activity. (A) Antibiogram assay with plugs of colonies (5 x 10 spores) grown on NMMP with different iron concentrations (10 nM, 4 M, and 2 mM) against *S. epidermidis, M. luteus,* and *E. coli*. (B) Comparison of inhibition halo diameters produced by *S. coelicolor* M145 (wt) and Δ*bfr* mutant against *S. epidermidis* (left) and *M. luteus* (right). Error bars show the standard error of the mean of the experiments carried out in triplicate. Asterisks show statistical differences between the two strains in the two iron concentrations compared: *: $p<0.05$; **: $p<0.01$ (two-way ANOVA).

Supplementary Material 8: Proteomics study. (A) Growth of *S. coelicolor* M145 (wt) and Δ*bfr* mutant on cellophane disks on LB medium at 3 and 4 days (conditions and times used for the proteomics study). (B) Volcano plots showing the abundance ratio (X axis) and the statistical significance (Y axis) of the more abundant (red) and less abundant (blue) proteins in the Δ*bfr* mutant detected at day 3 (left) and 4 (right). The horizontal light blue line shows the statistical threshold (adjusted *p*-value = 0.05).

Supplementary Material 9: Principal Component Analysis (PCA) of the proteomics study. PCA of proteins extracts from both strains (wt and Δ*bfr*) and time points (3 and 4 days).

Supplementary Material 10: Proteins linked to oxidative respiration and oxidative stress detected in the proteomic study. Proteins marked with * were only detected at day 3 and those marked with # were only detected at day 4. Represented ratios are the mean for proteins detected at both days. (A) Abundance ratios of proteins linked to respiration. (B) Abundance ratios of proteins linked to oxidative stress.

Supplementary Material 11: Proteins linked to cellular envelope and osmotic stress, and transporters, detected in the proteomics study. Proteins marked with * were only detected at day 3, and those marked with # were only detected at day 4. Represented ratios are the mean for proteins detected at both days. (A) Abundance ratios of transporters and proteins linked to cellular envelope stress. (B) Abundance ratios of proteins linked to osmotic stress.

Supplementary Material 12: Proteins linked to primary metabolism and nucleic acids processing detected in the proteomic study. Proteins marked with * were only detected at day 3 and those marked with # were only detected at day 4. Represented ratios are the mean for proteins detected at both days. (A) Abundance ratios of proteins linked to primary metabolism. (B) Abundance ratios of proteins linked to DNA processing and RNA translation.

Supplementary Material 13: Proteins identified with an adjusted *p*-value lower than 0.05 at day 3.

Supplementary Material 14: Proteins identified in with an adjusted *p*-value lower than 0.05 at day 4.

Acknowledgements
This work has been funded by projects PID2019-107716RB-I00 (financed by por MCIN/AEI /10.13039/501100011033) and PID2022-140962OB-I00 (financed by MCIN/AEI /10.13039/501100011033/ and by FEDER "Una manera de hacer Europa"). In addition, our institute, Institute of Functional Biology and Genomics (IBFG), is funded by the Program "Escalera de Excelencia" of the Junta de Castilla y León Ref. CLU-2017-03 Co-funded by the P.O. FEDER of Castilla y León 14-20; and the Internationalization Project "CL-EI-2021-08 - IBFG Unit of Excellence" of the CSIC, funded by the Junta de Castilla y León and co-financed by the European Union (ERDF "Europe drives our growth)". JGM has been funded by the the Regional Government of Castile and Leon/FEDER program ("Escalera de Excelencia" CLU-2017-03/14-20) of the IBFG, by the call for pre-doctoral contracts of University of Salamanca 2021, co-financed by Banco Santander, and by the aid for University teacher training FPU 2022 from Spanish Ministry of Education, Culture and Sport [FPU22/00747]. Also, we would like to thank Emma Keck for her help with the English language editing.

Author contributions
JG and LG conducted the experiments. JG, RIS and MD conceived the experiments and wrote the manuscript. All authors read and approved the final manuscript.

Data availability
The mass spectrometry proteomics data have been deposited to the ProteomeXchange Consortium viathe PRIDE partner repository with the dataset identifier PXD050869 and 10.6019/PXD050869.

Declarations

Ethics approval and consent to participate
Not applicable.

Consent for publication
Not applicable.

Competing interests
The authors declare no competing interests.

Received: 26 April 2024 / Accepted: 15 August 2024
Published online: 24 August 2024

References

1. Oren A, Garrity GM. Valid publication of the names of forty-two phyla of prokaryotes. Int J Syst Evol Microbiol. 2021;71(10).
2. Barka EA, Vatsa P, Sánchez L, Gaveau-Vaillant N, Jacquard C, Klenk HP, et al. Taxonomy, physiology, and Natural products of Actinobacteria. Microbiol Mol Biol Rev. 2016;80(1):1–43.
3. Beroigui O, Errachidi F. *Streptomyces* at the heart of several sectors to support practical and sustainable applications: a review. Prog Microbes Mol Biol. 2023;6.
4. van der Heul HU, Bilyk BL, McDowall KJ, Seipke RF, van Wezel GP. Regulation of antibiotic production in Actinobacteria: new perspectives from the post-genomic era. Nat Prod Rep. 2018;35(6):575–604.
5. Locatelli FM, Goo KS, Ulanova D. Effects of trace metal ions on secondary metabolism and the morphological development of streptomycetes. Metallomics. 2016;8(5):469–80.
6. Coisne S, Bechet M, Blondeau R. Actinorhodin production by *Streptomyces coelicolor A3(2)* in iron-restricted media. Lett Appl Microbiol. 1999;28(3):199–202.
7. Kim W, Hwang S, Lee N, Lee Y, Cho S, Palsson B, et al. Transcriptome and translatome profiles of *Streptomyces* species in different growth phases. Sci Data. 2020;7(1):138.
8. Tierrafría VH, Ramos-Aboites HE, Gosset G, Barona-Gómez F. Disruption of the siderophore-binding *desE* receptor gene in *Streptomyces coelicolor* A3(2) results in impaired growth in spite of multiple iron-siderophore transport systems. Microb Biotechnol. 2011;4(2):275–85.
9. Gesheva V, Ivanova V, Gesheva R. Effects of nutrients on the production of AK-111-81 macrolide antibiotic by *Streptomyces hygroscopicus*. Microbiol Res. 2005;160(3):243–8.
10. Jones SE, Pham CA, Zambri MP, McKillip J, Carlson EE, Elliot MA. *Streptomyces* Volatile compounds Influence Exploration and Microbial Community Dynamics by Altering Iron availability. MBio. 2019;10(2).
11. Senges CHR, Al-Dilaimi A, Marchbank DH, Wibberg D, Winkler A, Haltli B, et al. The secreted metabolome of *Streptomyces chartreusis* and implications for bacterial chemistry. Proc Natl Acad Sci U S A. 2018;115(10):2490–5.

12. Andrews SC, Robinson AK, Rodríguez-Quiñones F. Bacterial iron homeostasis. FEMS Microbiol Rev. 2003;27(2–3):215–37.
13. Bunet R, Brock A, Rexer HU, Takano E. Identification of genes involved in siderophore transport in *Streptomyces coelicolor* A3(2). FEMS Microbiol Lett. 2006;262(1):57–64.
14. Lensbouer JJ, Patel A, Sirianni JP, Doyle RP. Functional characterization and metal ion specificity of the metal-citrate complex transporter from *Streptomyces coelicolor*. J Bacteriol. 2008;190(16):5616–23.
15. Barona-Gómez F, Lautru S, Francou FX, Leblond P, Pernodet JL, Challis GL. Multiple biosynthetic and uptake systems mediate siderophore-dependent iron acquisition in *Streptomyces coelicolor* A3(2) and *Streptomyces ambofaciens* ATCC 23877. Microbiology. 2006;152(Pt 11):3355–66.
16. Khare G, Nangpal P, Tyagi AK. Differential roles of Iron Storage proteins in maintaining the Iron Homeostasis in *Mycobacterium tuberculosis*. PLoS ONE. 2017;12(1):e0169545.
17. Bradley JM, Svistunenko DA, Wilson MT, Hemmings AM, Moore GR, Le Brun NE. Bacterial iron detoxification at the molecular level. J Biol Chem. 2020;295(51):17602–23.
18. Wedderhoff I, Kursula I, Groves MR, Ortiz de Orue Lucana D. Iron binding at specific sites within the octameric HbpS protects streptomycetes from iron-mediated oxidative stress. PLoS ONE. 2013;8(8):e71579.
19. Lee EJ, Karoonuthaisiri N, Kim HS, Park JH, Cha CJ, Kao CM, et al. A master regulator sigmaB governs osmotic and oxidative response as well as differentiation via a network of sigma factors in *Streptomyces coelicolor*. Mol Microbiol. 2005;57(5):1252–64.
20. Faddetta T, Renzone G, Vassallo A, Rimini E, Nasillo G, Buscarino G, et al. *Streptomyces coelicolor* vesicles: many molecules to be delivered. Appl Environ Microbiol. 2022;88(1):e0188121.
21. Facey PD, Hitchings MD, Saavedra-García P, Fernández-Martínez L, Dyson PJ, Del Sol R. *Streptomyces coelicolor* dps-like proteins: differential dual roles in response to stress during vegetative growth and in nucleoid condensation during reproductive cell division. Mol Microbiol. 2009;73(6):1186–202.
22. Orban K, Finkel SE. Dps is a universally conserved dual-action DNA-Binding and Ferritin Protein. J Bacteriol. 2022;204(5):e0003622.
23. Hitchings MD, Townsend P, Pohl E, Facey PD, Jones DH, Dyson PJ, et al. A tale of tails: deciphering the contribution of terminal tails to the biochemical properties of two dps proteins from *Streptomyces coelicolor*. Cell Mol Life Sci. 2014;71(24):4911–26.
24. Busche T, Winkler A, Wedderhoff I, Ruckert C, Kalinowski J. Ortíz De Orué Lucana D. Deciphering the transcriptional response mediated by the redox-sensing aystem HbpS-SenS-SenR from *Streptomycetes*. PLoS ONE. 2016;11(8):e0159873.
25. Honarmand Ebrahimi K, Hagedoorn PL, Hagen WR. Unity in the biochemistry of the iron-storage proteins ferritin and bacterioferritin. Chem Rev. 2015;115(1):295–326.
26. Macedo S, Romao CV, Mitchell E, Matias PM, Liu MY, Xavier AV, et al. The nature of the di-iron site in the bacterioferritin from *Desulfovibrio desulfuricans*. Nat Struct Biol. 2003;10(4):285–90.
27. Eshelman K, Yao H, Punchi Hewage AND, Deay JJ, Chandler JR, Rivera M. Inhibiting the BfrB:Bfd interaction in *Pseudomonas aeruginosa* causes irreversible iron accumulation in bacterioferritin and iron deficiency in the bacterial cytosol. Metallomics. 2017;9(6):646–59.
28. Jobichen C, Ying Chong T, Rattinam R, Basak S, Srinivasan M, Choong YK, et al. Bacterioferritin nanocage structures uncover the biomineralization process in ferritins. PNAS Nexus. 2023;2(7):pgad235.
29. Tunca S, Barreiro C, Coque JJ, Martín JF. Two overlapping antiparallel genes encoding the iron regulator DmdR1 and the Adm proteins control siderophore and antibiotic biosynthesis in *Streptomyces coelicolor* A3(2). FEBS J. 2009;276(17):4814–27.
30. Cheng Y, Yang R, Lyu M, Wang S, Liu X, Wen Y, et al. IdeR, a DtxR family iron response regulator, controls iron homeostasis, morphological differentiation, secondary metabolism, and the oxidative stress response in *Streptomyces avermitilis*. Appl Environ Microbiol. 2018;84(22):e01503–18.
31. Rodríguez H, Rico S, Díaz M, Santamaría RI. Two-component systems in *Streptomyces*: key regulators of antibiotic complex pathways. Microb Cell Fact. 2013;12:127.
32. de la Sánchez R, Santamaría RI, Díaz M. Two-Component systems of *Streptomyces coelicolor*: an intricate network to be unraveled. Int J Mol Sci. 2022;23(23):15085.
33. Rico S, Santamaría RI, Yepes A, Rodríguez H, Laing E, Bucca G, et al. Deciphering the regulon of *Streptomyces coelicolor* AbrC3, a positive response regulator of antibiotic production. Appl Environ Microbiol. 2014a;80(8):2417–28.
34. Antoraz S, Rico S, Rodríguez H, Sevillano L, Alzate JF, Santamaría RI, et al. The Orphan Response Regulator Aor1 is a new relevant Piece in the Complex Puzzle of *Streptomyces coelicolor* Antibiotic Regulatory Network. Front Microbiol. 2017;8:2444.
35. de la Sánchez R, Antoraz S, Alzate JF, Santamaría RI, Díaz M. Antibiotic production and antibiotic resistance: the two sides of AbrB1/B2, a two-component system of *Streptomyces coelicolor*. Front Microbiol. 2020;11:587750.
36. MacNeil DJ, Gewain KM, Ruby CL, Dezeny G, Gibbons PH, MacNeil T. Analysis of *Streptomyces avermitilis* genes required for avermectin biosynthesis utilizing a novel integration vector. Gene. 1992;111(1):61–8.
37. Sambrook J, Fritsch E, Maniatis T. Molecular cloning: a laboratory manual. 2nd ed. Cold Spring Harbor, N. Y.: Cold Spring Harbor Laboratory; 1989.
38. Rose MD, Winston F, Hieter P. Methods in yeast genetics: a laboratory course manual. New York: Cold Spring Harbour Laboratory.; 1990.
39. Kieser T, Hopwood DA, Bibb JM, Chater KF, Buttner MJ. Practical *Streptomyces* genetics. Norwich, UK: John Innes Foundation; 2000.
40. Bentley SD, Chater KF, Cerdeño-Tárraga AM, Challis GL, Thomson NR, James KD, et al. Complete genome sequence of the model actinomycete *Streptomyces coelicolor A3*(2). Nature. 2002;417(6885):141–7.
41. Celis AI, Relman DA, Huang KC. The impact of iron and heme availability on the healthy human gut microbiome *in vivo* and *in vitro*. Cell Chem Biol. 2023;30(1):110–26. e3.
42. Green MR, Sambrook J. Molecular cloning: a laboratory manual (Fourth Edition). Cold Spring Harbor Laboratory Press. Cold Spring Harbor, New York; 2012.
43. Kuhstoss S, Richardson MA, Rao RN. Plasmid cloning vectors that integrate site-specifically in *Streptomyces* spp. Gene. 1991;97(1):143–6.
44. Fernández-Abalos JM, Reviejo V, Díaz M, Rodríguez S, Leal F, Santamaría RI. Posttranslational processing of the xylanase Xys1L from *Streptomyces halstedii* JM8 is carried out by secreted serine proteases. Microbiology. 2003;149:1623–32.
45. Santamaría RI, Martínez-Carrasco A, de la Sánchez R, Torres-Vila LM, Bonal R, Martín J et al. Characterization of actinomycetes strains isolated from the intestinal tract and feces of the larvae of the longhorn beetle *Cerambyx Welensii*. Microorganisms. 2020;8(12).
46. CRISPy. Cas9 target finder for S. coelicolor. http://staff.biosustain.dtu.dk/laeb/crispy_scoeli/
47. Ronda C, Pedersen LE, Hansen HG, Kallehauge TB, Betenbaugh MJ, Nielsen AT, et al. Accelerating genome editing in CHO cells using CRISPR Cas9 and CRISPy, a web-based target finding tool. Biotechnol Bioeng. 2014;111(8):1604–16.
48. Tong Y, Charusanti P, Zhang L, Weber T, Lee SY. CRISPR-Cas9 based engineering of actinomycetal genomes. ACS Synth Biol. 2015.
49. Yepes A, Rico S, Rodríguez-García A, Santamaría RI, Díaz M. Novel two-component systems implied in antibiotic production in *Streptomyces coelicolor*. PLoS ONE. 2011;6(5):e19980.
50. Gottelt M, Kol S, Gómez-Escribano JP, Bibb M, Takano E. Deletion of a regulatory gene within the *cpk* gene cluster reveals novel antibacterial activity in *Streptomyces coelicolor* A3(2). Microbiology. 2010;156(Pt 8):2343–53.
51. Abbasi U, Abbina S, Gill A, Bhagat V, Kizhakkedathu JN. A facile colorimetric method for the quantification of labile iron pool and total iron in cells and tissue specimens. Sci Rep. 2021;11(1):6008.
52. Fish WW. Rapid colorimetric micromethod for the quantitation of complexed iron in biological samples. Methods Enzymol. 1988;158:357–64.
53. Punchi Hewage AND, Fontenot L, Guidry J, Weldeghiorghis T, Mehta AK, Donnarumma F et al. Mobilization of Iron Stored in Bacterioferritin is required for metabolic homeostasis in *Pseudomonas aeruginosa*. Pathogens. 2020;9(12).
54. CNB. Proteomics Facility http://proteo.cnb.csic.es/proteomica
55. Deutsch EW, Bandeira N, Pérez-Riverol Y, Sharma V, Carver JJ, Mendoza L, et al. The ProteomeXchange consortium at 10 years: 2023 update. Nucleic Acids Res. 2023;51(D1):D1539–48.
56. Pérez-Riverol Y, Bai J, Bandla C, García-Seisdedos D, Hewapathirana S, Kamatchinathan S, et al. The PRIDE database resources in 2022: a hub for mass spectrometry-based proteomics evidences. Nucleic Acids Res. 2022;50(D1):D543–52.
57. Pérez-Riverol Y, Xu QW, Wang R, Uszkoreit J, Griss J, Sanchez A, et al. PRIDE Inspector Toolsuite: moving toward a Universal Visualization Tool for Proteomics Data Standard Formats and Quality Assessment of ProteomeXchange Datasets. Mol Cell Proteom. 2016;15(1):305–17.
58. StrepDB. The *Streptomyces* Annotation Server https://strepdb.streptomyces.org.uk/

59. Szklarczyk D, Kirsch R, Koutrouli M, Nastou K, Mehryary F, Hachilif R, et al. The STRING database in 2023: protein-protein association networks and functional enrichment analyses for any sequenced genome of interest. Nucleic Acids Res. 2023;51(D1):D638–46.
60. STRING. database https://string-db.org/
61. Shannon P, Markiel A, Ozier O, Baliga NS, Wang JT, Ramage D, et al. Cytoscape: a software environment for integrated models of biomolecular interaction networks. Genome Res. 2003;13(11):2498–504.
62. Google-Scholar. https://scholar.google.es/
63. Uniprot. https://www.uniprot.org/
64. UniProt C. UniProt: the universal protein knowledgebase in 2021. Nucleic Acids Res. 2021;49(D1):D480–9.
65. NCBI. Conserved Domain Database. https://www.ncbi.nlm.nih.gov/Structure/cdd/wrpsb.cgi/
66. Lu S, Wang J, Chitsaz F, Derbyshire MK, Geer RC, Gonzales NR, et al. CDD/SPARCLE: the conserved domain database in 2020. Nucleic Acids Res. 2020;48(D1):D265–8.
67. KEGG. Kyoto Encyclopedia of Genes and Genomes. https://www.kegg.jp/
68. Kanehisa M, Furumichi M, Tanabe M, Sato Y, Morishima K. KEGG: new perspectives on genomes, pathways, diseases and drugs. Nucleic Acids Res. 2017;45(D1):D353–61.
69. DAVID. Database for Annotation, Visualization and Integrated Discovery. https://david.ncifcrf.gov/
70. Sherman BT, Hao M, Qiu J, Jiao X, Baseler MW, Lane HC, et al. DAVID: a web server for functional enrichment analysis and functional annotation of gene lists (2021 update). Nucleic Acids Res. 2022;50(W1):W216–21.
71. Tang J, Zhu Z, He H, Liu Z, Xia Z, Chen J, et al. Bacterioferritin: a key iron storage modulator that affects strain growth and butenyl-spinosyn biosynthesis in *Saccharopolyspora Pogona*. Microb Cell Fact. 2021;20(1):157.
72. Yang J, Pan X, Xu Y, Li Y, Xu N, Huang Z, et al. *Agrobacterium tumefaciens* ferritins play an important role in full virulence through regulating iron homeostasis and oxidative stress survival. Mol Plant Pathol. 2020;21(9):1167–78.
73. Shi M, Wan F, Mao Y, Gao H. Unraveling the mechanism for the viability deficiency of *Shewanella oneidensis oxyR* null mutant. J Bacteriol. 2015;197(13):2179–89.
74. Lee N, Kim W, Chung J, Lee Y, Cho S, Jang KS, et al. Iron competition triggers antibiotic biosynthesis in *Streptomyces coelicolor* during coculture with *Myxococcus xanthus*. ISME J. 2020;14(5):1111–24.
75. Hassett RF, Romeo AM, Kosman DJ. Regulation of high affinity iron uptake in the yeast *Saccharomyces cerevisiae.* Role of dioxygen and Fe. J Biol Chem. 1998;273(13):7628–36.
76. Lejeune C, Sago L, Cornu D, Redeker V, Virolle MJ. A proteomic analysis indicates that oxidative stress is the common feature triggering antibiotic production in *Streptomyces coelicolor* and in the *pptA* mutant of *Streptomyces lividans*. Front Microbiol. 2022;12:813993.
77. Li C, Li L, Huang L, Li A. Pleiotropic effects of ActVI-ORFA as an unusual regulatory factor identified in the biosynthetic pathway of actinorhodin in *Streptomyces coelicolor*. Microbiol Res. 2021;250:126792.
78. Mo S, Sydor PK, Corre C, Alhamadsheh MM, Stanley AE, Haynes SW, et al. Elucidation of the *Streptomyces coelicolor* pathway to 2-undecylpyrrole, a key intermediate in undecylprodiginine and streptorubin B biosynthesis. Chem Biol. 2008;15(2):137–48.
79. Cerdeño AM, Bibb MJ, Challis GL. Analysis of the prodiginine biosynthesis gene cluster of *Streptomyces coelicolor* A3(2). New mechanisms for chain initiation and termination in modular multienzymes. Chem Biol. 2001;8:818–29.
80. Bednarz B, Kotowska M, Pawlik KJ. Multi-level regulation of coelimycin synthesis in *Streptomyces coelicolor* A3(2). Appl Microbiol Biotechnol. 2019;103(16):6423–34.
81. Swiatek-Polatynska MA, Bucca G, Laing E, Gubbens J, Titgemeyer F, Smith CP, et al. Genome-wide analysis of in vivo binding of the master regulator DasR in *Streptomyces coelicolor* identifies novel non-canonical targets. PLoS ONE. 2015;10(4):e0122479.
82. Wang LY, Li ST, Li Y. Identification and characterization of a new exopolysaccharide biosynthesis gene cluster from *Streptomyces*. FEMS Microbiol Lett. 2003;220(1):21–7.
83. Kol S, Merlo ME, Scheltema RA, de Vries M, Vonk RJ, Kikkert NA, et al. Metabolomic characterization of the salt stress response in *Streptomyces coelicolor*. Appl Environ Microbiol. 2010;76(8):2574–81.
84. Jiang J, He X, Cane DE. Biosynthesis of the earthy odorant geosmin by a bifunctional *Streptomyces coelicolor* enzyme. Nat Chem Biol. 2007;3(11):711–5.
85. Biarnes-Carrera M, Lee CK, Nihira T, Breitling R, Takano E. Orthogonal regulatory circuits for *Escherichia coli* based on the gamma-butyrolactone system of *Streptomyces coelicolor*. ACS Synth Biol. 2018;7(4):1043–55.
86. Li YQ, Chen PL, Chen SF, Wu D, Zheng J. A pair of two-component regulatory genes ecrA1/A2 in S. coelicolor. J Zhejiang Univ Sci. 2004;5(2):173–9.
87. Thomas L, Hodgson DA, Wentzel A, Nieselt K, Ellingsen TE, Moore J, et al. Metabolic switches and adaptations deduced from the proteomes of *Streptomyces coelicolor* wild type and *phoP* mutant grown in batch culture. Mol Cell Proteom. 2012;11(2):M111013797.
88. Hoskisson PA, Hutchings MI. MtrAB-LpqB: a conserved three-component system in actinobacteria? Trends Microbiol. 2006;14(10):444–9.
89. Zhang P, Wu L, Zhu Y, Liu M, Wang Y, Cao G, et al. Deletion of MtrA inhibits cellular development of *Streptomyces coelicolor* and alters expression of developmental regulatory genes. Front Microbiol. 2017;8:2013.
90. Som NF, Heine D, Holmes N, Knowles F, Chandra G, Seipke RF, et al. The MtrAB two-component system controls antibiotic production in *Streptomyces coelicolor* A3(2). Microbiology. 2017;163(10):1415–9.
91. Hindra PP, Elliot MA. Regulation of a novel gene cluster involved in secondary metabolite production in *Streptomyces coelicolor*. J Bacteriol. 2010;192(19):4973–82.
92. Riascos C, Martínez-Carrasco A, Díaz M, Santamaría RI. Role of fourteen XRE-DUF397 pairs from *Streptomyces coelicolor* as regulators of antibiotic production and differentiation. New players in a complex regulatory network. Front Microbiol. 2023;14:1217350.
93. Zhang L, Li WC, Zhao CH, Chater KF, Tao MF. NsdB, a TPR-like-domain-containing protein negatively affecting production of antibiotics in *Streptomyces coelicolor* A3 (2). Wei Sheng Wu Xue Bao. 2007;47(5):849–54.
94. Saito N, Xu J, Hosaka T, Okamoto S, Aoki H, Bibb MJ, et al. EshA accentuates ppGpp accumulation and is conditionally required for antibiotic production in *Streptomyces coelicolor* A3(2). J Bacteriol. 2006;188(13):4952–61.
95. Komatsu M, Takano H, Hiratsuka T, Ishigaki Y, Shimada K, Beppu T, et al. Proteins encoded by the conservon of *Streptomyces coelicolor* A3(2) comprise a membrane-associated heterocomplex that resembles eukaryotic G protein-coupled regulatory system. Mol Microbiol. 2006;62(6):1534–46.
96. Takano H, Hashimoto K, Yamamoto Y, Beppu T, Ueda K. Pleiotropic effect of a null mutation in the *cvn1* conservon of *Streptomyces coelicolor* A3(2). Gene. 2011;477(1–2):12–8.
97. Bonet B, Ra Y, Cantu Morin LM, Soto Bustos J, Livny J, Traxler MF. The cvn8 conservon system is a global regulator of specialized metabolism in *Streptomyces* coelicolor during interspecies linteractions. mSystems. 2021;6(5):e0028121.
98. Castro-Melchor M, Charaniya S, Karypis G, Takano E, Hu WS. Genome-wide inference of regulatory networks in *Streptomyces coelicolor*. BMC Genomics. 2010;11(1):578.
99. Finn D, Catton K, Heenan M, Kopittke PM, Ouwerkerk D, Klieve AV, et al. Differential gene expression in the model actinomycete *Streptomyces coelicolor* A3(2) supports nitrogen mining dependent on the plant carbon to nitrogen ratio. Agriculture. 2018;8(12):192.
100. Dela Cruz R, Gao Y, Penumetcha S, Sheplock R, Weng K, Chander M. Expression of the *Streptomyces coelicolor* SoxR regulon is intimately linked with actinorhodin production. J Bacteriol. 2010;192(24):6428–38.
101. Shin JH, Singh AK, Cheon DJ, Roe JH. Activation of the SoxR regulon in *Streptomyces coelicolor* by the extracellular form of the pigmented antibiotic actinorhodin. J Bacteriol. 2011;193(1):75–81.
102. Falke D, Fischer M, Biefel B, Ihling C, Hammerschmidt C, Reinefeld K, et al. Cytochrome bcc-aa3 oxidase supercomplexes in the aerobic respiratory chain of *Streptomyces coelicolor* A3(2). J Mol Microbiol Biotechnol. 2019;28(6):255–68.
103. Guo H, Suzuki T, Rubinstein JL. Structure of a bacterial ATP synthase. Elife. 2019;8.
104. Urem M, van Rossum T, Bucca G, Moolenaar GF, Laing E, Swiatek-Polatynska MA, et al. OsdR of *Streptomyces coelicolor* and the dormancy regulator DevR of *Mycobacterium tuberculosis* control overlapping regulons. mSystems. 2016;1(3):e00014–16.
105. Aldridge M, Facey P, Francis L, Bayliss S, Del Sol R, Dyson P. A novel bifunctional histone protein in *Streptomyces*: a candidate for structural coupling between DNA conformation and transcription during development and stress? Nucleic Acids Res. 2013;41(9):4813–24.
106. Lyzen R, Maitra A, Milewska K, Kochanowska-Lyzen M, Hernández VJ, Szalewska-Palasz A. The dual role of DksA protein in the regulation of *Escherichia coli pArgX* promoter. Nucleic Acids Res. 2016;44(21):10316–25.

107. Travis BA, Schumacher MA. Diverse molecular mechanisms of transcription regulation by the bacterial alarmone ppGpp. Mol Microbiol. 2022;117(2):252–60.
108. Daigle F, Lerat S, Bucca G, Sanssouci E, Smith CP, Malouin F, et al. A terD domain-encoding gene (*SCO2368*) is involved in calcium homeostasis and participates in calcium regulation of a DosR-like regulon in *Streptomyces coelicolor*. J Bacteriol. 2015;197(5):913–23.
109. Fischer M, Falke D, Ronitz J, Haase A, Damelang T, Pawlik T, et al. Hypoxia-induced synthesis of respiratory nitrate reductase 2 of *Streptomyces coelicolor* A3(2) depends on the histidine kinase OsdK in mycelium but not in spores. Microbiol (Reading). 2019;165(8):905–16.
110. Falke D, Biefel B, Haase A, Franke S, Fischer M, Sawers RG. Activity of spore-specific respiratory nitrate reductase 1 of *Streptomyces coelicolor* A3(2) requires a functional cytochrome bcc-aa 3 oxidase supercomplex. J Bacteriol. 2019;201(11).
111. Honma S, Ito S, Yajima S, Sasaki Y. Nitric oxide signaling for actinorhodin production in *Streptomyces coelicolor* A3(2) via the DevS/R two-component system. Appl Environ Microbiol. 2021;87(14):e00480–21.
112. Sasaki Y, Oguchi H, Kobayashi T, Kusama S, Sugiura R, Moriya K, et al. Nitrogen oxide cycle regulates nitric oxide levels and bacterial cell signaling. Sci Rep. 2016;6:22038.
113. Nakajima S, Satoh Y, Yanashima K, Matsui T, Dairi T. Ergothioneine protects *Streptomyces coelicolor* A3(2) from oxidative stresses. J Biosci Bioeng. 2015;120(3):294–8.
114. Yoshizumi T, Shibui Y, Kogo M, Honma S, Ito S, Yajima S, et al. Mycothiol maintains the homeostasis and signalling of nitric oxide in *Streptomyces coelicolor* A. BMC Microbiol. 2023;3(2):M145.
115. Kim MS, Dufour YS, Yoo JS, Cho YB, Park JH, Nam GB, et al. Conservation of thiol-oxidative stress responses regulated by SigR orthologues in actinomycetes. Mol Microbiol. 2012;85(2):326–44.
116. Hahn JS, Oh SY, Roe JH. Role of OxyR as a peroxide-sensing positive regulator in *Streptomyces coelicolor* A3(2). J Bacteriol. 2002;184(19):5214–22.
117. Manteca A, Jung HR, Schwammle V, Jensen ON, Sánchez J. Quantitative proteome analysis of *Streptomyces coelicolor* nonsporulating liquid cultures demonstrates a complex differentiation process comparable to that occurring in sporulating solid cultures. J Proteome Res. 2010;9(9):4801–11.
118. Tran NT, Huang X, Hong HJ, Bush MJ, Chandra G, Pinto D, et al. Defining the regulon of genes controlled by sigma(E), a key regulator of the cell envelope stress response in *Streptomyces coelicolor*. Mol Microbiol. 2019;112(2):461–81.
119. Hesketh A, Hill C, Mokhtar J, Novotna G, Tran N, Bibb M, et al. Genome-wide dynamics of a bacterial response to antibiotics that target the cell envelope. BMC Genomics. 2011;12:226.
120. Li F, Liang J, Wang W, Zhou X, Deng Z, Wang Z. Analysis of *Streptomyces coelicolor* membrane proteome using two-dimensional native/native and native/sodium dodecyl sulfate gel electrophoresis. Anal Biochem. 2014;465:148–55.
121. Alonso-Fernández S, Arribas-Díez I, Fernández-García G, González-Quiñonez N, Jensen ON, Manteca A. Quantitative phosphoproteome analysis of *Streptomyces coelicolor* by immobilized zirconium (IV) affinity chromatography and mass spectrometry reveals novel regulated protein phosphorylation sites and sequence motifs. J Proteom. 2022;269:104719.
122. Dulermo T, Lejeune C, Aybeke E, Abreu S, Bleton J, David M, et al. Genome analysis of a variant of *Streptomyces coelicolor* M145 with high lipid content and poor ability to synthetize antibiotics. Microorganisms. 2023;11(6):1470.
123. Facey PD, Sevcikova B, Novakova R, Hitchings MD, Crack JC, Kormanec J, et al. The *dpsA* gene of *Streptomyces coelicolor*: induction of expression from a single promoter in response to environmental stress or during development. PLoS ONE. 2011;6(9):e25593.
124. Lee EJ, Cho YH, Kim HS, Ahn BE, Roe JH. Regulation of sigmaB by an anti- and an anti-anti-sigma factor in *Streptomyces coelicolor* in response to osmotic stress. J Bacteriol. 2004;186(24):8490–8.
125. Kormanec J, Sevcikova B, Novakova R, Homerova D, Rezuchova B, Mingyar E. The complex roles and regulation of stress response σ factors in *Streptomyces coelicolor*. Stress and environmental regulation of gene expression and adaptation in bacteria. John Wiley & Sons Inc.; 2016. pp. 328–43.
126. Lee EJ, Cho YH, Kim HS, Roe JH. Identification of sigmab-dependent promoters using consensus-directed search of *Streptomyces coelicolor* genome. J Microbiol. 2004;42(2):147–51.
127. Sevcikova B, Rezuchova B, Mazurakova V, Homerova D, Novakova R, Feckova L, et al. Cross-recognition of promoters by the nine SigB homologues present in *Streptomyces coelicolor* A3(2). Int J Mol Sci. 2021;22(15):7849.
128. Kim HS, Lee EJ, Cho YH, Roe JH. Post-translational regulation of a developmental catalase, CatB, involves a metalloprotease, SmpA and contributes to proper differentiation and osmoprotection of *Streptomyces coelicolor*. Res Microbiol. 2013;164(4):327–34.
129. Yagüe P, Rodríguez-García A, López-García MT, Martín JF, Rioseras B, Sánchez J, et al. Transcriptomic analysis of *Streptomyces coelicolor* differentiation in solid sporulating cultures: first compartmentalized and second multinucleated mycelia have different and distinctive transcriptomes. PLoS ONE. 2013;8(3):e60665.
130. Sexton DL, St-Onge RJ, Haiser HJ, Yousef MR, Brady L, Gao C, et al. Resuscitation-promoting factors are cell wall-lytic enzymes with important roles in the germination and growth of *Streptomyces coelicolor*. J Bacteriol. 2015;197(5):848–60.
131. Bibb MJ, Domonkos A, Chandra G, Buttner MJ. Expression of the chaplin and rodlin hydrophobic sheath proteins in *Streptomyces* venezuelae is controlled by sigma(BldN) and a cognate anti-sigma factor, RsbN. Mol Microbiol. 2012;84(6):1033–49.
132. den Hengst CD, Tran NT, Bibb MJ, Chandra G, Leskiw BK, Buttner MJ. Genes essential for morphological development and antibiotic production in *Streptomyces coelicolor* are targets of BldD during vegetative growth. Mol Microbiol. 2010;78(2):361–79.
133. Elliot MA, Bibb MJ, Buttner MJ, Leskiw BK. BldD is a direct regulator of key developmental genes in *Streptomyces coelicolor A3*(2). Mol Microbiol. 2001;40(1):257–69.
134. Vladimirov M, Zhang RX, Mak S, Nodwell JR, Davidson AR. A contractile injection system is required for developmentally regulated cell death in *Streptomyces coelicolor*. Nat Commun. 2023;14(1):1469.
135. Kim ES, Song JY, Kim DW, Chater KF, Lee KJ. A possible extended family of regulators of sigma factor activity in *Streptomyces coelicolor*. J Bacteriol. 2008;190(22):7559–66.
136. Mingyar E, Sevcikova B, Rezuchova B, Homerova D, Novakova R, Kormanec J. The sigma(F)-specific anti-sigma factor RsfA is one of the protein kinases that phosphorylates the pleiotropic anti-anti-sigma factor BldG in *Streptomyces coelicolor* A3(2). Gene. 2014;538(2):280–7.
137. Ulanova D, Kitani S, Fukusaki E, Nihira T. SdrA, a new DeoR family regulator involved in *Streptomyces avermitilis* morphological development and antibiotic production. Appl Environ Microbiol. 2013;79(24):7916–21.
138. Haiser HJ, Yousef MR, Elliot MA. Cell wall hydrolases affect germination, vegetative growth, and sporulation in *Streptomyces* coelicolor. J Bacteriol. 2009;191(21):6501–12.
139. Tian Y, Fowler K, Findlay K, Tan H, Chater KF. An unusual response regulator influences sporulation at early and late stages in *Streptomyces coelicolor*. J Bacteriol. 2007;189(7):2873–85.
140. Bagchi S, Tomenius H, Belova LM, Ausmees N. Intermediate filament-like proteins in bacteria and a cytoskeletal function in *Streptomyces*. Mol Microbiol. 2008;70(4):1037–50.
141. Eccleston M, Willems A, Beveridge A, Nodwell JR. Critical residues and novel effects of overexpression of the *Streptomyces coelicolor* developmental protein BldB: evidence for a critical interacting partner. J Bacteriol. 2006;188(23):8189–95.
142. Swiatek MA, Gubbens J, Bucca G, Song E, Yang YH, Laing E, et al. The ROK-family regulator Rok7B7 pleiotropicaly affects xylose utilization, carbon catabolite repression and antibiotic production in *Streptomyces coelicolor*. J Bacteriol. 2013;195:1236–48.
143. Saito A, Fujii T, Shinya T, Shibuya N, Ando A, Miyashita K. The *msiK* gene, encoding the ATP-hydrolysing component of N,N′-diacetylchitobiose ABC transporters, is essential for induction of chitinase production in *Streptomyces coelicolor* A3(2). Microbiology. 2008;154(Pt 11):3358–65.
144. Viens P, Dubeau MP, Kimura A, Desaki Y, Shinya T, Shibuya N, et al. Uptake of chitosan-derived D-glucosamine oligosaccharides in *Streptomyces coelicolor* A3(2). FEMS Microbiol Lett. 2015;362(9):fnv048.
145. Temuujin U, Chi WJ, Chang YK, Hong SK. Identification and biochemical characterization of Sco3487 from *Streptomyces coelicolor* A3(2), an exo- and endo-type beta-agarase-producing neoagarobiose. J Bacteriol. 2012;194(1):142–9.
146. Diacovich L, Peiru S, Kurth D, Rodríguez E, Podesta F, Khosla C, et al. Kinetic and structural analysis of a new group of Acyl-CoA carboxylases found in *Streptomyces coelicolor* A3(2). J Biol Chem. 2002;277(34):31228–36.
147. Revill WP, Bibb MJ, Scheu AK, Kieser HJ, Hopwood DA. Beta-ketoacyl acyl carrier protein synthase III (FabH) is essential for fatty acid biosynthesis in *Streptomyces coelicolor* A3(2). J Bacteriol. 2001;183(11):3526–30.
148. Brzostek A, Rumijowska-Galewicz A, Dziadek B, Wojcik EA, Dziadek J. ChoD and HsdD can be dispensable for cholesterol degradation in mycobacteria. J Steroid Biochem Mol Biol. 2013;134:1–7.

149. Schniete JK, Reumerman R, Kerr L, Tucker NP, Hunter IS, Herron PR, et al. Differential transcription of expanded gene families in central carbon metabolism of *Streptomyces coelicolor* A3(2). Access Microbiol. 2020;2(6):acmi000122.
150. Tiffert Y, Franz-Wachtel M, Fladerer C, Nordheim A, Reuther J, Wohlleben W, et al. Proteomic analysis of the GlnR-mediated response to nitrogen limitation in *Streptomyces coelicolor* M145. Appl Microbiol Biotechnol. 2011;89(4):1149–59.
151. Pérez-Redondo R, Rodríguez-García A, Botas A, Santamarta I, Martín JF, Liras P. ArgR of *Streptomyces coelicolor* is a versatile regulator. PLoS ONE. 2012;7(3):e32697.
152. Zhang L, Nguyen HC, Chipot L, Piotrowski E, Bertrand C, Thibessard A, et al. The *adnAB* locus, encoding a putative helicase-nuclease activity, is essential in *Streptomyces*. J Bacteriol. 2014;196(14):2701–8.
153. Cordeiro T, Gontijo MTP, Jorge GP, Brocchi M. EbfC/YbaB: a widely distributed nucleoid-associated protein in prokaryotes. Microorganisms. 2022;10(10).
154. Fornelos N, Browning DF, Butala M. The use and abuse of LexA by mobile genetic elements. Trends Microbiol. 2016;24(5):391–401.
155. Rico S, Yepes A, Rodríguez H, Santamaría J, Antoraz S, Krause EM, et al. Regulation of the AbrA1/A2 two-component system in *Streptomyces coelicolor* and the potential of its deletion strain as a heterologous host for antibiotic production. PLoS ONE. 2014b;9(10):e109844.
156. Yagüe P, Rodríguez-García A, López-García MT, Rioseras B, Martín JF, Sánchez J, et al. Transcriptomic analysis of liquid non-sporulating *Streptomyces coelicolor* cultures demonstrates the existence of a complex differentiation comparable to that occurring in solid sporulating cultures. PLoS ONE. 2014;9(1):e86296.
157. Oliveira FM, Da Costa AC, Procopio VO, García W, Araujo JN, Da Silva RA, et al. *Mycobacterium abscessus* subsp. *massiliense mycma_0076* and *mycma_0077* genes code for ferritins that are modulated by iron concentration. Front Microbiol. 2018;9:1072.
158. Expert D, Boughammoura A, Franza T. Siderophore-controlled iron assimilation in the enterobacterium *Erwinia chrysanthemi*: evidence for the involvement of bacterioferritin and the Suf iron-sulfur cluster assembly machinery. J Biol Chem. 2008;283(52):36564–72.
159. Flores FJ, Martín JF. Iron-regulatory proteins DmdR1 and DmdR2 of *Streptomyces coelicolor* form two different DNA-protein complexes with iron boxes. Biochem J. 2004;380(Pt 2):497–503.
160. Figueiredo MC, Lobo SA, Carita JN, Nobre LS, Saraiva LM. Bacterioferritin protects the anaerobe *Desulfovibrio vulgaris Hildenborough* against oxygen. Anaerobe. 2012;18(4):454–8.
161. Ma JF, Ochsner UA, Klotz MG, Nanayakkara VK, Howell ML, Johnson Z, et al. Bacterioferritin A modulates catalase A (KatA) activity and resistance to hydrogen peroxide in *Pseudomonas aeruginosa*. J Bacteriol. 1999;181(12):3730–42.
162. Bitoun JP, Wu G, Ding H. Escherichia coli FtnA acts as an iron buffer for re-assembly of iron-sulfur clusters in response to hydrogen peroxide stress. Biometals. 2008;21(6):693–703.
163. Velayudhan J, Castor M, Richardson A, Main-Hester KL, Fang FC. The role of ferritins in the physiology of *Salmonella enterica* Sv. *Typhimurium*: a unique role for ferritin B in iron-sulphur cluster repair and virulence. Mol Microbiol. 2007;63(5):1495–507.
164. Stewart MYY, Bush MJ, Crack JC, Buttner MJ, Le Brun NE. Interaction of the *Streptomyces* Wbl protein WhiD with the principal sigma factor sigma(HrdB) depends on the WhiD [4Fe-4S] cluster. J Biol Chem. 2020;295(28):9752–65.
165. Lee KL, Yoo JS, Oh GS, Singh AK, Roe JH. Simultaneous activation of iron- and thiol-based sensor-regulator systems by redox-active compounds. Front Microbiol. 2017;8:139.
166. Kim JS, Lee HN, Kim P, Lee HS, Kim ES. Negative role of *wblA* in response to oxidative stress in *Streptomyces coelicolor*. J Microbiol Biotechnol. 2012;22(6):736–41.
167. Aubert C, Mandin P, Py B. Mrp and SufT, two bacterial homologs of eukaryotic CIA factors involved in Fe-S clusters biogenesis. Inorganics. 2023;11(11):431.
168. Zheng C, Dos Santos PC. Metallocluster transactions: dynamic protein interactions guide the biosynthesis of Fe-S clusters in bacteria. Biochem Soc Trans. 2018;46(6):1593–603.
169. Virolle MJ. A challenging view: antibiotics play a role in the regulation of the energetic metabolism of the producing bacteria. Antibiot (Basel). 2020;9(2):83.
170. Singh AK, Shin JH, Lee KL, Imlay JA, Roe JH. Comparative study of SoxR activation by redox-active compounds. Mol Microbiol. 2013;90(5):983–96.

Publisher's note